FINITE ELEMENT ANALYSIS OF A DEEP DRAWING PROCESS

A THESIS SUBMITTED IN PARTIAL FULFILLMENT OF THE REQUIREMENT FOR THE AWARD OF THE DEGREE OF

MASTER OF TECHNOLOGY
(COMPUTATIONAL DESIGN)
TO

DELHI TECHNOLOGICAL UNIVERSITY

SUBMITTED BY

KUNAL MATHUR
ROLL NO.: 2K13/CDN/18

UNDER THE GUIDANCE OF

DR. ATUL KUMAR AGRAWAL
ASSOCIATE PROFESSOR

MR. VIJAY GAUTAM
ASSISTANT PROFESSOR

DEPARTMENT OF MECHANICAL, PRODUCTION & INDUSTRIAL AND AUTOMOBILE ENGINEERING
DELHI TECHNOLOGICAL UNIVERSITY
BAWANA ROAD, DELHI-110042

2016

DELHI TECHNOLOGICAL UNIVERSITY

(Formerly Delhi College of Engineering)

Shahbad Daulatpur, Bawana Road,

Delhi-110042

STUDENT'S DECLARATION

I, **Kunal Mathur,** hereby declare that the work which is being presented in this thesis entitled **"Finite Element Analysis of a Deep Drawing Process"** submitted in the partial fulfillment of the requirement for degree of **Master of Technology (Computational Design)** in Department of Mechanical Engineering at **Delhi Technological University** is an authentic record of my own work carried out under the supervision of **Associate Prof. Atul Kumar Agrawal and Assistant Prof. Vijay Gautam.** The matter presented in this thesis has not been submitted in any other University/Institute for the award of Master of Technology Degree. Also, it has not been directly copied from any source without giving its proper reference.

Signature of Student

DELHI TECHNOLOGICAL UNIVERSITY

(Formerly Delhi College of Engineering)

Shahbad Daulatpur, Bawana Road,

Delhi-110042

CERTIFICATE

This is to certify that this thesis report entitled, **"Finite Element Analysis of a Deep Drawing Process"** being submitted by **Kunal Mathur (Roll No. 2K13/CDN/18)** at Delhi Technological University, Delhi for the award of the Degree of Master of Technology as per academic curriculum. It is a record of bonafide research work carried out by the student under my supervision and guidance, towards partial fulfillment of the requirement for the award of Master of Technology degree in Computational Design. The work is original as it has not been submitted earlier in part or full for any purpose before.

Dr. Atul Kumar Agrawal
Associate Professor

Mr. Vijay Gautam
Assistant Professor

Department of Mechanical Engineering

Delhi Technological University

Delhi-110042

ACKNOWLEDGEMENT

First and foremost, praises and thanks to the God, the Almighty, for His showers of blessings throughout my research work to complete the research successfully.

I would like to extend my gratitude to **Prof. R. S. Mishra, Head,** Department of Mechanical Engineering, Delhi Technological University, for providing this opportunity to carry out the present thesis work.

I would like to express my deep and sincere gratitude to my research supervisors, **Associate Prof. Atul Kumar Agrawal** and **Assistant Prof. Vijay Gautam,** Department of Mechanical Engineering, Delhi Technological University, for their continuous support, patience, motivation, enthusiasm, and immense knowledge which have always been a constant source of motivation for me. Their excellent guidance, perseverance, invaluable suggestions made this work possible and complete. It was a great privilege and honor to work and study under their guidance. Without their wise advice and able guidance, it would have been impossible to complete the thesis in this manner.

I am extremely grateful to my parents, family and friends for their love, prayers, caring and sacrifices for educating and preparing me for my future.

KUNAL MATHUR
M.Tech. (COMPUTATIONAL DESIGN)
2K13/CDN/18

ABSTRACT

Sheet metal forming has an important place in the manufacturing industry because of the wide range of ready to use products that it manufactures. Components with smooth surfaces associated to the low cost per part, due to the high rate of production, are the main factors which make this process the first choice for the industry. Traditionally, experimental procedures have been employed to determine these changes and adjust process settings (dies, loadings, tool path) accordingly. However, this approach is time consuming and depends heavily on the experience of the tool designer. With the advent of fast computing, sheet metal forming simulations have gained popularity.

Present work analyses a deep drawing process of a tapered product using Altair Hyperform. A 3-D FEM simulation model has been developed using Altair Hyperform to study the effects of various deep drawing variables such as die and punch radii, blank holder pressure on the quality of drawn components. Forming Limit Diagrams and thinning percentage contours generated by the software are analyzed to study wrinkling and possibility of tearing, the two major defects associated with deep drawn components.

It has been observed that a tapered product can be easily drawn with Limiting Drawing Ratios greater than 2, something which is very difficult in case of straight cylindrical products. The results from the simulation have shown that the product formed after varying different variables such as die radius and blank holder pressure is of good quality.

Key Words: Deep Drawing, tapered product, high limiting drawing ratio, wrinkling, thinning, Altair Hyperform.

TABLE OF CONTENTS

LIST OF FIGURES

LIST OF TABLES

CHAPTER 1

INTRODUCTION

1.1 Overview of Metal Forming Technology

About 85% of all metal used in various industrial fields is processed through casting operation to obtain simple product forms like ingots and slabs, and these products go through further deformation operations to arrive at the stage of becoming final usable products **[1]**.

Metal forming includes a wide range of manufacturing processes in which the metal workpiece undergoes a plastic change in the shape by the application of external forces by means of various forming tools. It is very important to distinguish between the terms "deforming" and "forming". In the case of uncontrolled plastic straining, the term "deforming" should be used whereas the term "forming" should be used with controlled plastic strain to gain a specific shape for the product **[2]**.

In metal forming processes that use forming tools, usually called dies, stresses exceeding the yield strength of the metal are generated in the processed workpiece. The metal hence deforms producing the desired shape as guided by the forming tools. A successful metal forming operation indicates that the plastic deformation of the workpiece occurs without material failure. However, flowing of the metal into the forming die is not easy because the deformation occurs in the solid state. Therefore, it is necessary to take into consideration, not only the laws of material behaviour but also the ductility of material and pressure, forces and power requirements while designing a metal working process. In addition, continuous interactions between material properties and process conditions play a crucial role in the success of a metal forming process **[1]**. All of the shaping processes such as solidification processes, formation processes and material removal, are generally classified under the title of metal forming technology **[3]**.

Metal forming processes are classified into bulk deformation processes and sheet metal forming processes, where the former refers to the category of processes that change the shape/size of the workpiece extensively, and the latter refers to the category of processes performed on metallic sheets, whose thickness lies in the range of 0.4mm to 6mm.

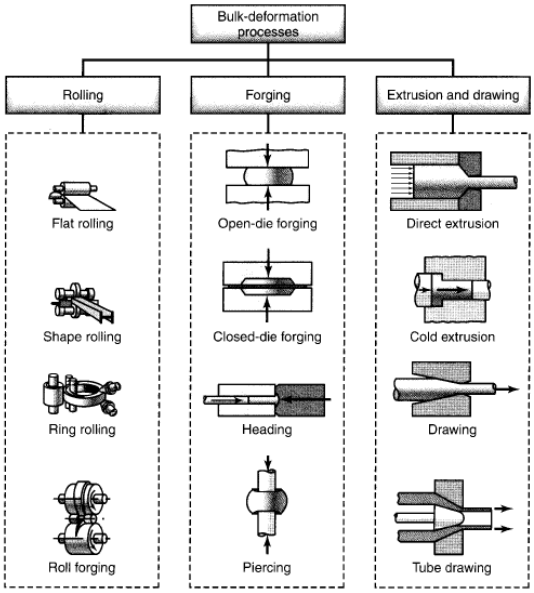

Fig. 1.1: Schematic illustrations of various bulk-deformation processes.[4]

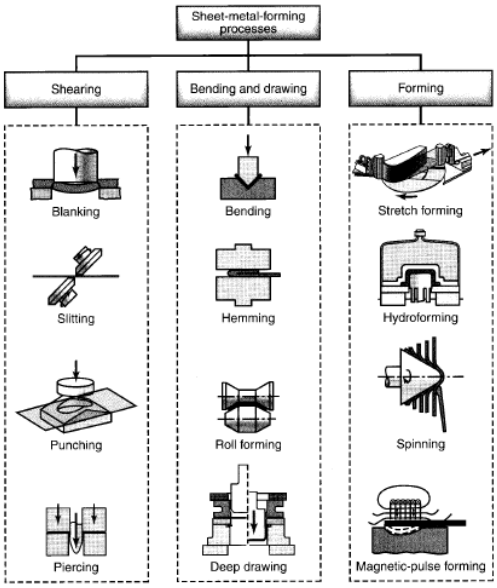

Fig. 1.2: Schematic illustrations of various sheet-metal-forming processes. [4]

1.2 Sheet Metal Forming Processes

Sheet metal forming can be generally identified by cutting and forming operations performed on metallic sheets. In order to distinguish between the terms "sheet" and "plate", it is important to realize that the range of sheet thickness is typically from 0.4mm to 6mm, while the term plate usually refers to the product of thickness greater than 6mm. The work metal used in sheet metal forming, whether sheet or plate is produced by rolling, hence the significant importance of sheet metal forming outlines the importance of the rolling process. Traditionally sheet is available as coils if it is thin; otherwise it is supplied as flat sheet or plate. Sheet metal parts are utilized in different industrial applications such as automobile and truck bodies, aircraft, railway cars, farm and construction equipment, beverage cans, kitchen utensils, etc.[3]

Unlike the bulk forming processes, the major characteristic of sheet metal forming is the use of a workpiece with high ratio of surface area to thickness. In sheet metal forming, tensile forces are mainly utilized in the plane of the sheet to achieve the process, whereas compressive forces that are generated in the transverse direction as a result of the tension may result in folding or wrinkling of the sheet. As a result, any reduction in the thickness is due to

tensile stress induced in the sheet itself. Therefore, the most important concern in all sheet metal forming processes is to avoid excessive decreasing in thickness, which can lead to necking and fracture **[3, 5]**. Usually most of the sheets forming processes are carried out at room temperature (cold processing conditions) excepting if the work piece is thick; the sheet metal is brittle or the deformation is massive.

1.3 Overview of Deep Drawing Process

Deep drawing is one of the most commonly used sheet metal forming processes. It is defined as a manufacturing process in which a sheet metal work piece known as blank is subjected to tensile and compressive stresses by the action of a mechanical punch to press the blank into a die cavity as seen in figure 1.3. The process is capable of producing final work pieces that generate little scrap material with enough precision for the parts to be straightaway assembled without further operations. Deep drawing is widely used in the manufacturing industry also because of its rapid cycle times. Complex geometries, not necessarily axisymmetrical, can be produced with a few operations which are automatable and thus require a relatively non-technical workforce. Deep drawing has been developed at a fast rate, especially in the automotive and aircraft industries. Typical products are cylindrical, conical or box-shaped parts such as containers, kitchen sinks, beverage cans, pans and automotive panels. The raw material required should be ductile for the manufacturing process but tough and strong for the products to be of practical use.

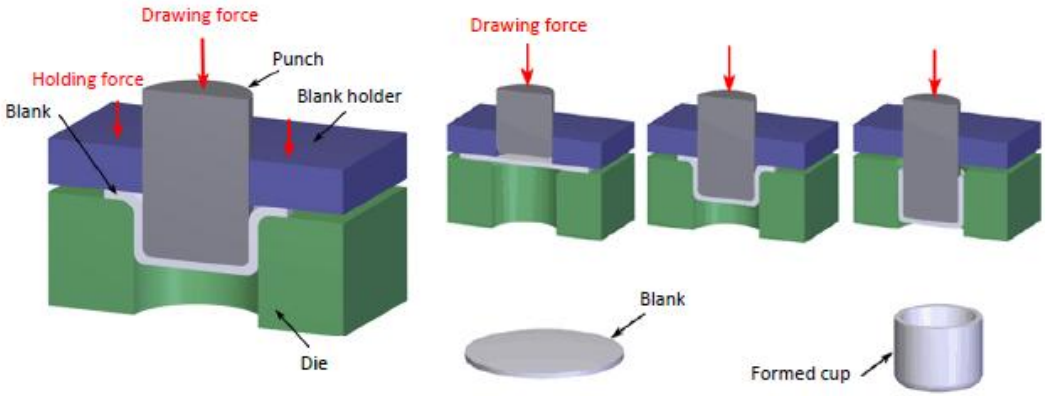

Fig. 1.3: Schematic illustration of deep drawing process.

Fig. 1.4: Some deep drawn parts

1.4 Objectives

Sheet metal processes, especially deep drawing is an important manufacturing process as many parts with complex geometries used in automotive and aircraft applications are being manufactured by these sheet metal processes. Deep drawing is a complex process and the end product depends on many variables such as die radius, punch radius and blank holder pressure, which need to be studied. This study aims to simulate the deep drawing process of a part used in the automobile industry as a bracket for coil spring in the car door assembly using Altair Hyperform 11.0. Forming Limit Diagrams produced by the software as well as the thinning percentage contours will be studied to predict the quality of the deep drawn component.

1.5 Organization of Thesis

The chapters of the thesis are arranged in the following manner. *Chapter one* presents the background of this project along with the objectives. The primary aim of this chapter is to provide the reader with a basic idea of the work presented in the thesis. *Chapter two* provides a comprehensive literature review related to various aspects of the deep drawing process. *Chapter three* describes the deep drawing process in detail. *Chapter four* deals with the modeling of the components and simulation of various stages of deep drawing. *Chapter five* provides the results obtained by the simulation study. Finally, *Chapter six* concludes the thesis and provides suggestions for future work.

CHAPTER 2

LITERATURE REVIEW

With an aim to summarise the different technical concepts that are utilized in the deep drawing process as well as to reveal the influence of the key process parameters on the quality of drawn products, a literature review is presented in this chapter.

Hill. R. [6] analyzed the pure radial drawing of an annular flange assuming a rigid plastic material. He considered plane strain and plane stress cases. Frictional forces were considered negligible and the material was taken to be isotropic. The Tresca yield criterion was assumed with the Levy-Mises flow rule. He concluded that the generalized strain to be taken to be equal to the circumferential strain in the flange. He showed the positions of the particles in the deforming flange and proved that there was little dependence on the stress-strain properties of the material. There was greater tendency of work hardening and reduction of thickness of material across the annulus at any moment.

Chung S.Y. and Swift H.W. [7,8] extended the work to consider the friction at the rim of the blank. Their assumptions were justified by detailed comparison with their experimental work. Swift's work led to a good understanding of radial drawing and to an appreciation of thinning of material as it passes over the die. They reported punch load for different travel positions of punch. Chung and Swift pointed out that their theory is not capable of predicting strains over the punch head, where critical conditions generally occur leading to fracture. Their theory can be used for predicting punch loads and power requirements, however, although the computation is necessarily complicated and· is not recommended for general use.

Lankford W.T. et al [9] recognized the importance of the variation of r-value with orientation in the plane of sheet for commercial low carbon steel. They reported that the variation in r-values could be exploited for unsymmetrical stampings. The variation of the plastic behavior with direction is assessed by a quantity called Lankford parameter or anisotropy coefficient which is determined by uniaxial tensile tests on sheet specimens in the form of a strip. The anisotropy coefficient (r) is defined by

$$r = \frac{\epsilon_2}{\epsilon_3} \tag{2.1}$$

where ϵ_2 ; ϵ_3 are the strains in the width and thickness directions, respectively.

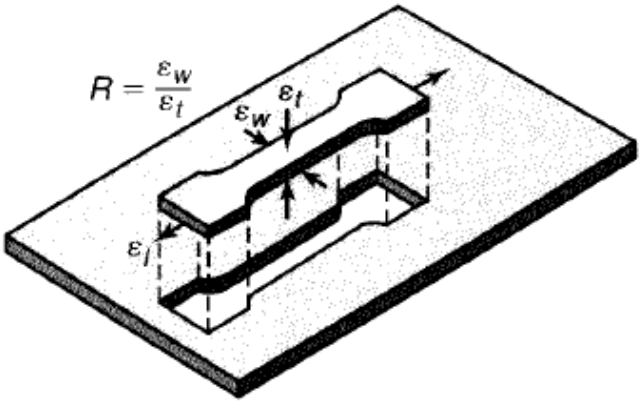

Fig. 2.1: Strains on a tensile-test specimen removed from a piece of sheet metal.

Equation 2.1 can also be written as

$$r = \frac{ln\frac{b}{b_o}}{ln\frac{t}{t_o}} \tag{2.2}$$

where b_o and b are the initial and final width, while t_o and t are the initial and final thickness of the specimen, respectively.

Taking into account the condition of volume constancy, $\epsilon_1 + \epsilon_2 + \epsilon_3 = 0$, following form of 2.1 is obtained

$$r = -\frac{\epsilon_1}{\epsilon_2+\epsilon_1} \tag{2.3}$$

and 2.2 becomes

$$r = \frac{-ln\frac{b}{b_0}}{ln\frac{l}{l_0} + ln\frac{b}{b_0}} \tag{2.4}$$

El-Sebaie M.G. et al [10] presented theoretical results of n and r on the limiting draw ratio when drawing with a flat headed punch. They concluded through experiments that n-value has little effect on limiting draw ratio and while increasing r-value increases the draw ratio. They have shown that at least two instability modes are possible. The first mode in the cup wall occurs under plane strain tension and is most likely to apply to annealed materials. The second mode is in the flange under uniaxial tension and this is most likely to apply to

materials that have been previously cold-worked. The limiting drawing ratios for drawing with rough punch are somewhat greater than those for drawing with smooth punch.

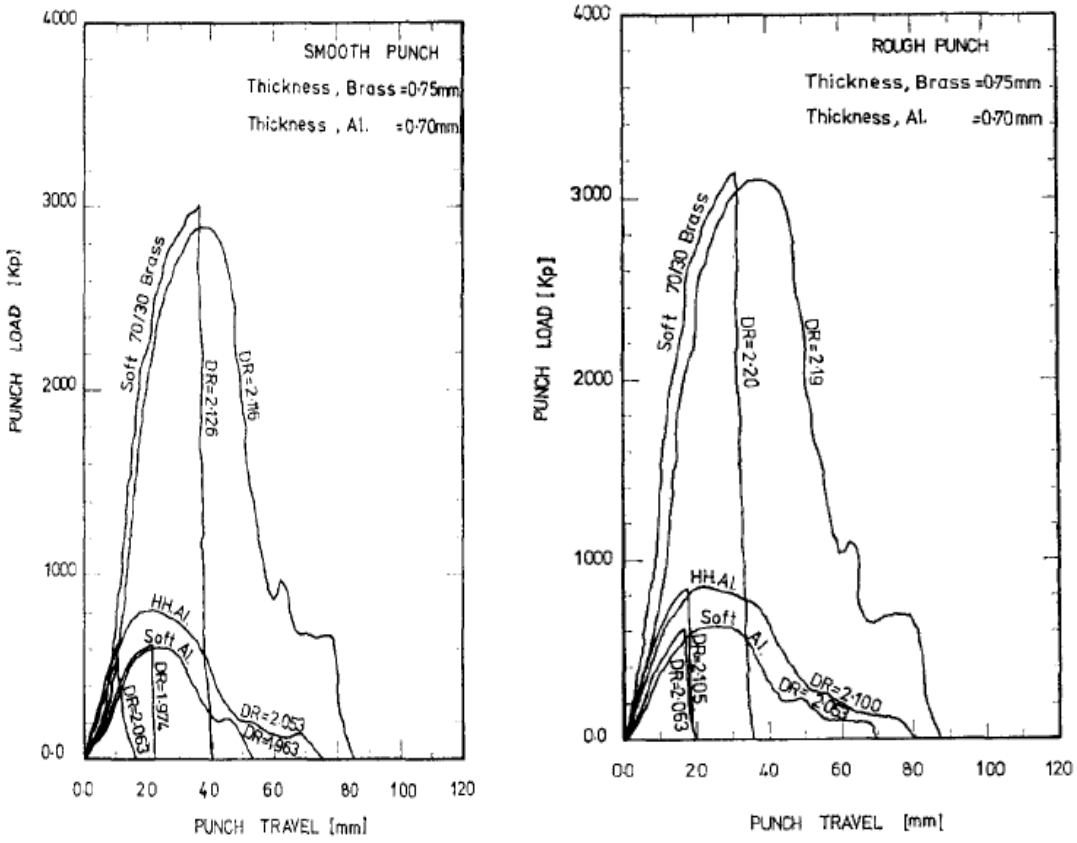

Fig. 2.2: Punch load/travel diagrams for all materials drawn with (a) smooth punch (b) rough punch

Darendeliler H. et al [11] developed finite element method to study elasto-plastic deformation of sheet materials in the presence of large strain and displacements. They have assumed the sheet material to be isotropic and insensitive which obeys J_2 flow theory. The work hardening characteristics of the material and Coulomb friction between sheet metal and punch were considered with a constant blank holding force.

Yang D.Y. and Lee H.S. [12] suggested that deformation region can be divided into several zones by considering geometric characteristics and contact boundary conditions. An elliptical punch was used and experimental results were compared with computed results and found to be in good agreement with experimental value for the punch load and thickness strain distributions.

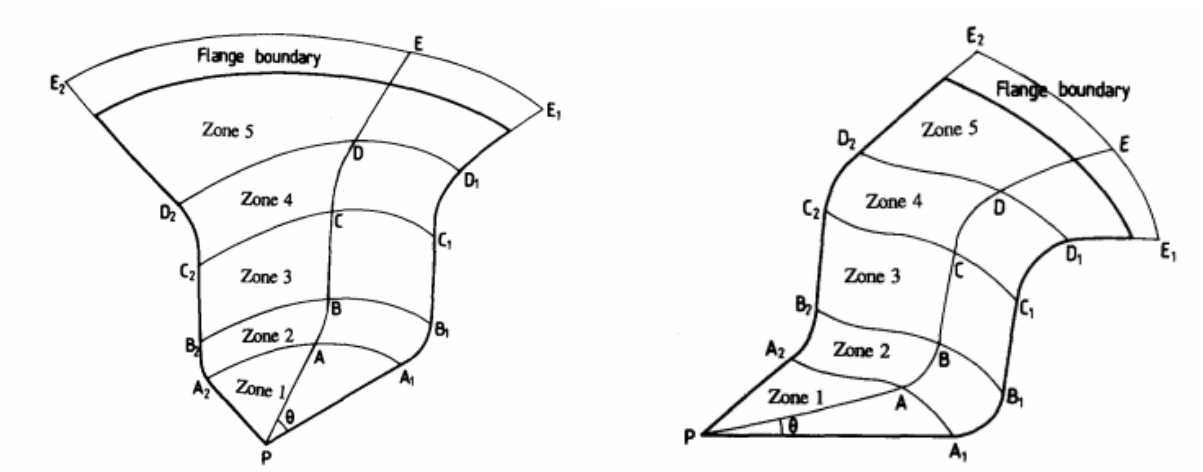

Fig. 2.3: (a) Schematic diagram of five regions in the deep drawing by an elliptical punch. (b)Schematic diagram of five regions in the deep drawing by a clover-type punch.

Lee C.H. and Kobayashi. S [13] described the matrix method for the analysis of rigid-plastic deformation problems and demonstrated its use to analyse simple compression of cylinders and plane stress hole expansion and flange drawing of planar anisotropic sheets. The matrix method enabled the computation of free surface barreling and produced the so-called "folding" that has been a long known fact but never shown by a theoretical calculation previously.

Seo [14] investigated the work hardening of the material during multiple forming. The thrust of his work was on the loss of ductility due to cumulative work hardening during multiple deep drawing. A three-dimensional model was used to conceptualize the design necessary to set up finite element models. The results of his work showed that work hardening induced from the first draw station affects material deformation behavior in subsequent forming. The aim of the investigation was to predict material fracture upon reaching a final shaping station.

Michal J. Saran et al [15] developed a formulation for numerical simulation of complex forming with special emphasis on accuracy and computational efficiency. An incremental displacement approach based on Lagrangian formulation with elastic visco-plastic material model with Hill's cross-anisotropy, power law hardening and strain rate sensitivity are assumed was attempted. Adaptive remeshing procedures were adopted which reduced the number of elements while maintaining the same level of accuracy. They concluded that strain distribution agrees with the experimental values.

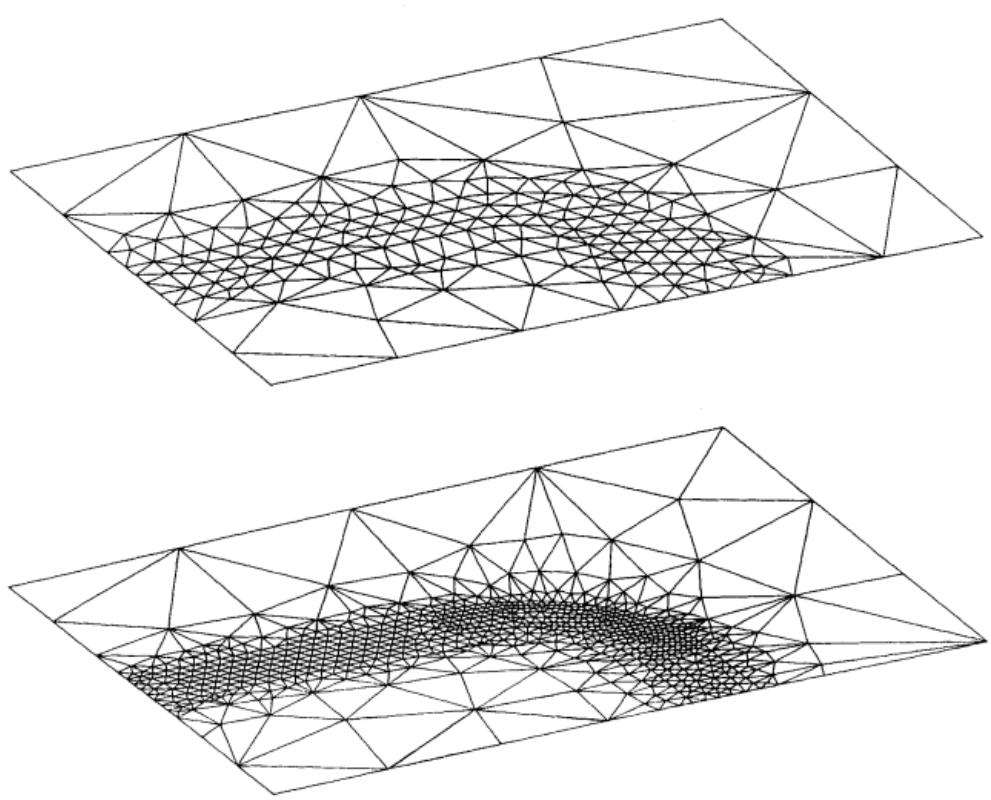

Fig. 2.4: Adaptively redesigned meshes for the test part example

Jain et al. [16] conducted simulations on the progressive-die-sequence design for automotive parts. The objectives of their investigation were to determine the number of forming stages, tool geometry for each stage, drawing depth in each forming stage and the blank holder force for each stage. They concluded that the integration of simulations and past experience can reduce the number of die tryout tests and associated time and cost. Furthermore, they concluded that integrating simulations allows further refinement and optimization of the die design to improve product properties such as wall thickness tolerances.

Keeler[17] pioneered the research in the field of Forming Limit Diagrams (FLDs). He demonstrated that the maximum values of the principal strains $\epsilon 1$and $\epsilon 2$ can be determined by measuring the strains at fracture on sheet components covered with grids of circles. During forming the initial circles of the grid become ellipses. Keeler plotted the maximum principal strain against the minimum principal strain obtained from such ellipses at fracture of parts after biaxial stretching ($\epsilon 1 > 0$; $\epsilon 2 > 0$) [18]. This way he obtained a curve limiting the tolerable range.

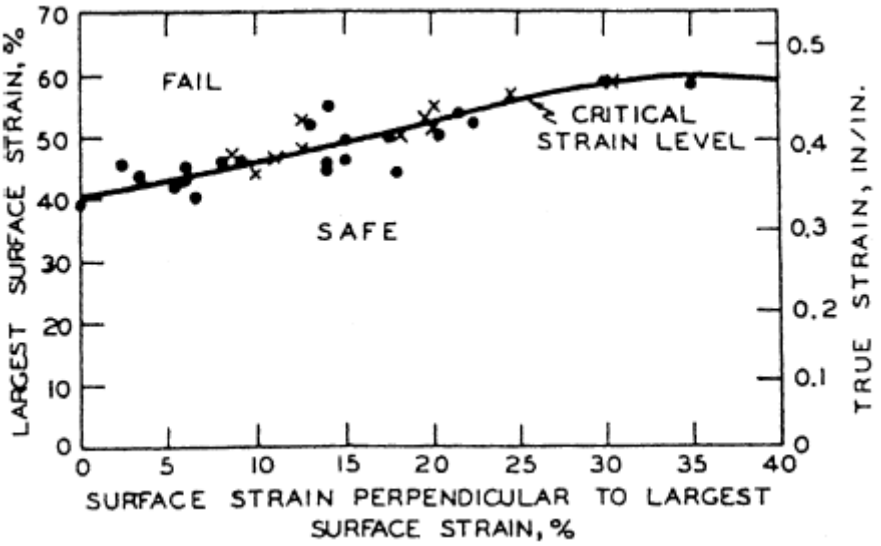

Fig. 2.5: Forming limit diagram defined by Keeler[17]

Goodwin [19] plotted the curve for the tension/compression domain ($\varepsilon 1 > 0$; $\varepsilon 2 < 0$) by using different mechanical tests. In this case, transverse compression allows for obtaining high values of tensile strains like in rolling or drawing.

The diagrams of Keeler (right side) and Goodwin (left side) are currently called the Forming Limit Diagram (FLD), see Fig.2.6.

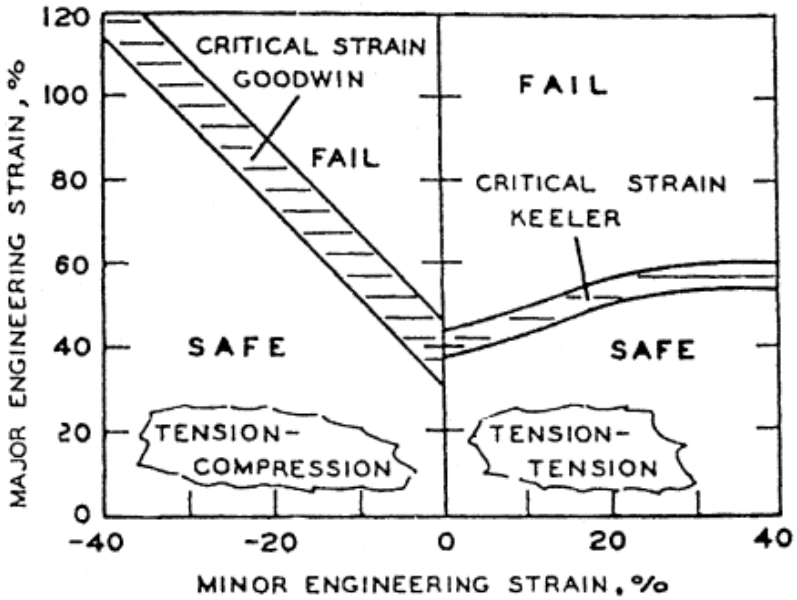

Fig. 2.6: Forming limit diagrams defined by Keeler and Goodwin [19]

Connecting all of the points corresponding to limit strains leads to a Forming Limit Curve (FLC). The FLC splits the 'fail' (i.e. above the FLC) and 'save' (i.e. below the FLC) regions. The Forming Limit Curve (FLC) is plotted on a Forming Limit Diagram (FLD). The intersection of the limit curve with the vertical axis (which represents the plane strain deformation ($\varepsilon 2 = 0$) is an important point of the FLD and is noted FLD_0.

Today, depending on the kind of limit strains that is measured different types of FLD's are determined: for necking and for fracture, see Fig. 2.7.

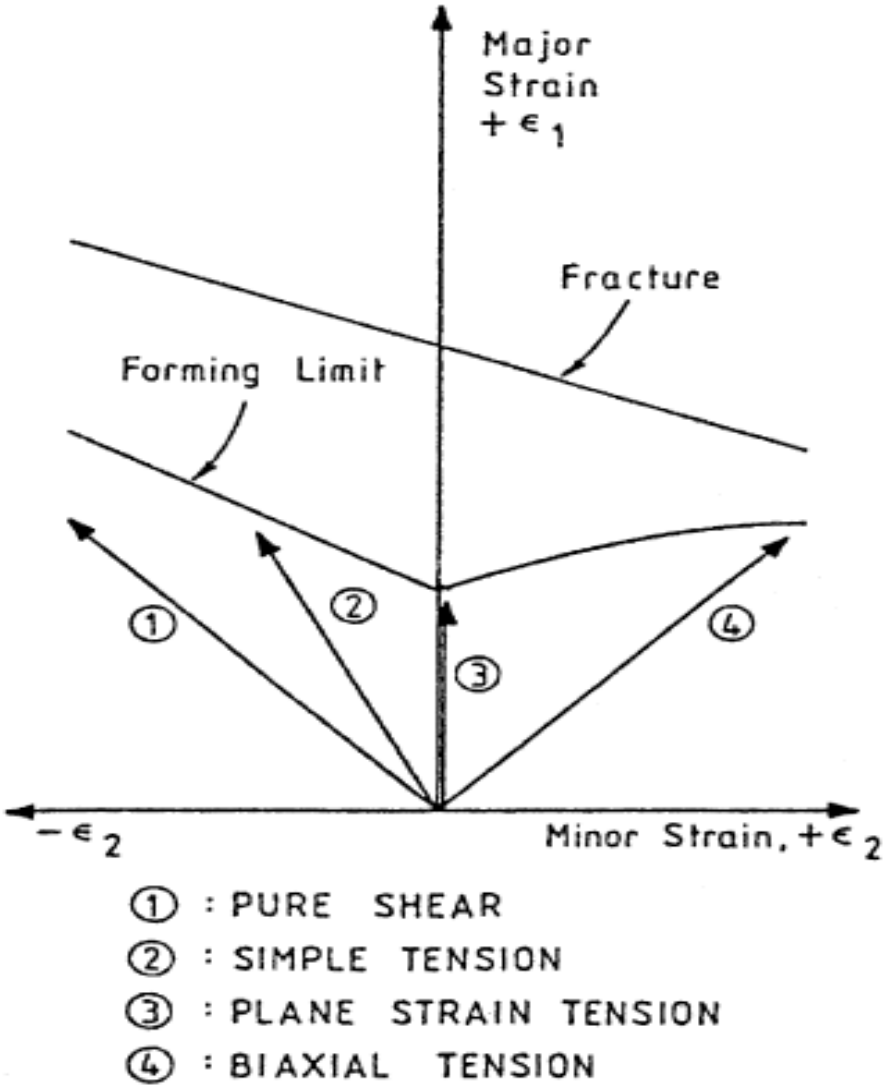

Fig. 2.7: Forming limit diagrams for necking and for fracture

Kaftanoglu [20] developed a method to model flange wrinkling in axisymmetrical deep drawing using the energy method. In this approach, wrinkling occurs if the plastic work done for deep drawing is higher than the plastic work done for wrinkling. For this purpose, using

von Mises yield criteria, a plastic analysis is done for the flange part of the blank, assuming plane stress conditions. For the calculation of work done for wrinkling, wrinkles are assumed to be a sine curve in shape. So the amplitude of the wrinkles are calculated, then using the plastic bending moment, work done for wrinkling is obtained. Using these procedures, plastic work versus reduction strain curves are obtained for both deep drawing and wrinkling. When the slope of the wrinkling curve is greater than deep drawing curve, wrinkling does not occur, since the energy required is greater than deep drawing. Considering the peaks of the wrinkles as plastic hinges, the blank-holder force needed to suppress wrinkling is found in terms of wave number. Experiments are conducted to verify the numerical results with several materials and for several initial blank diameters.

Ramaekers et al. [21], made a research on the deep drawability of a round cylindrical cup. The limiting drawing ratio is tried to be related with some process parameters like anisotropy factor, strain hardening exponent, etc… Upper and lower bound methods are used to obtain theoretical models. Using the theoretical model proposed for deep drawing, estimation for the limiting drawing ratio is tried to be achieved. Some experiments are conducted to verify the model developed. Comparing the results, it is seen that an agreement between the model for deep drawing and experiments. However, a precise prediction of the limiting drawing ratio could not be achieved. The friction coefficient is seen to be an important factor for the drawability of large size products. The study showed that decreasing friction coefficient, increases limiting drawing ratio.

Cao and Boyce [22] examined wrinkling and tearing type of failures in sheet metal forming. For prediction of wrinkling, they used a method proposed by Cao and Boyce. The criterion is based on the energy conservation and minimum work to suppress the wrinkling. Total strain energy values for a perfect plate and for buckling plate are recorded. Then the force/pressure needed to suppress the wrinkling is calculated using the energy difference and wrinkling amplitude. In prediction of tearing, existing forming limit diagrams are used in correspondence with the local strain histories near possible tearing regions. They also developed a technique named variable binder force in which blank–holding load varies in controlled manner, not a constant blank–holding load was used. A control algorithm is proposed for variable binder force technology. Two examples are used: conical cup drawing and square cup drawing. Finite element models of both cases are analyzed by commercial

program ABAQUS. Comparison with the experimental results shows that the method is capable of predicting wrinkling and tearing. The control algorithm for variable binder force is tried in both cases, and 16% extra cup forming height is provided for conical cup drawing.

Makinouchi et al [23] analyzed wrinkling during deep drawing of conical cups numerically and experimentally. The experiments were conducted not only to create a reference for FEM simulation, but also to give some guidelines for a reliable benchmark test of the wrinkling prediction capability of various FEM codes. The simple component geometry enabled the easy comparison of experimental and FEM results. To make numerical results more general, two types of FEM analyses were employed: static-explicit (ITAS3D) and dynamic-explicit (ABAQUS/Explicit). The same simulation parameters used enabled the comparison of both techniques. The experiments were carried out with an anisotropic sheet with a view to investigate the shape of wrinkles on a hydraulic press because of its advantage in controlling load and ram velocity which can be adjusted according to the requirements of the deformation process.

Ferron et al [24] developed a bifurcation analysis for predicting the occurrence of wrinkling in metal sheets with isotropic elasticity and transversely anisotropic plasticity. Based on the local conditions describing sheet geometry, loading and material anisotropy, wrinkling is predicted in the form of a limit curve defining bifurcation in principal stress space, along with the wavelength and orientation of the wrinkles. The practical relevance of this approach was checked by comparison with FE predictions of wall wrinkling in the conical cup test in the Abaqus, a FE code. The simulations are made for different materials.

Sherbiny et al [25] successfully simulated the deep drawing process as a required step to validate the quality of the tool design before implementation. For this purpose, a 3-D Finite Element (FE) model was developed using ABAQUS/EXPLICIT. The material is modeled as an elastic–plastic material with isotropic elasticity, using the Hill anisotropic yield criterion for the plasticity to describe the anisotropic characteristics of the sheet metal within the simulation programme. The FE results are compared with experimental results for validation. The developed model can predict the thickness distribution, thinning, and the maximum residual stresses of the blank at different die design parameters, including both geometrical

and physical parameters. Furthermore, it is used for predicting reliable, working parameters without expensive shop trials. Predictions of the thickness distribution, thinning and the maximum residual stresses of the sheet metal blank with different design parameters are reported. Frictional limitations and requirements at the different interfaces are also investigated.

Rees [26] examined the formability of a zinc clad automotive CR sheet steel. This material's extended ductility allows a diffuse instability condition to define the limit of formability at the onset of necking under in-plane biaxial stressing. It is shown how this theory can admit material anisotropy, sheet orientation, thickness, strain history and changes to its r and n values under any ratio of applied principal stresses. Shown here are the influences upon limiting formability of: (i) orientation between the principal stress axes and the sheet's rolling direction in 158 increments between 08 and 908; (ii) n-values between 0.1 and 0.3; (iii) r-values between 1.1 and 1.8; (iv) equivalent prestrains from -15 to +15%; (v) sheet thickness between 0.25 and 1.5 mm. The ratio between the in-plane principal stresses is allowed to vary between 0 and $\pm$1 for constructing two forming limit diagrams. These forming limit diagrams (FLDs) plot either the limiting in-plane principal engineering strains, eP1 versus eP2, or the major in-plane and thickness strains, eP1 versus eP3

Faraji et al [27] obtained an LDR of 9 in FE analysis of the multi-stage deep drawing carried out by ABAQUS/explicit FE code. Furthermore, to predict the onset of necking, the forming limit diagram and the forming limit stress diagram were computed and implemented into FE analysis. The best LDRs for each stage were obtained from FE analysis. Experimental tests were conducted based on FE analysis results for comparison purpose. Also, the wall thickness distributions obtained using the finite element method (FEM) was compared with results from several tests.

Choubey et al [28] simulated the deep drawing process with ANSYS 14.0 Software. The die and punch is assumed to be rigid and for the deformable Mild Steel blank, the elasto-plastic analysis is carried out. This way the concern of different process parameters such as coefficient of friction, punch pressure, blank-holder pressure is studied. The main objective of this study is to investigate the effects of Blank-holder pressure (BHP) on the quality of

deep drawn product. The effect of BHP variation on failure limits and the limiting drawing ratio in axisymmetric deep drawing operations are studied. Blank material is mild steel and finite element method is used for the simulation. The study includes many aspects that affect the final product.

CHAPTER 3

DEEP DRAWING PROCESS

3.1 Introduction

Drawing operation is the process of forming a flat piece of material (blank) of appropriate size into a hollow shape by means of a punch which causes the blank material to flow into the die-cavity. The depth of the draw may be **shallow, moderate** or **deep.** If the depth of the formed cup is upto half its diameter, the process is known as **Shallow Drawing.** If the depth of the formed cup exceeds the diameter, it is called **Deep Drawing**. Parts of various geometries and sizes are made by drawing operation, two extreme examples being bottle caps and automobile panels.

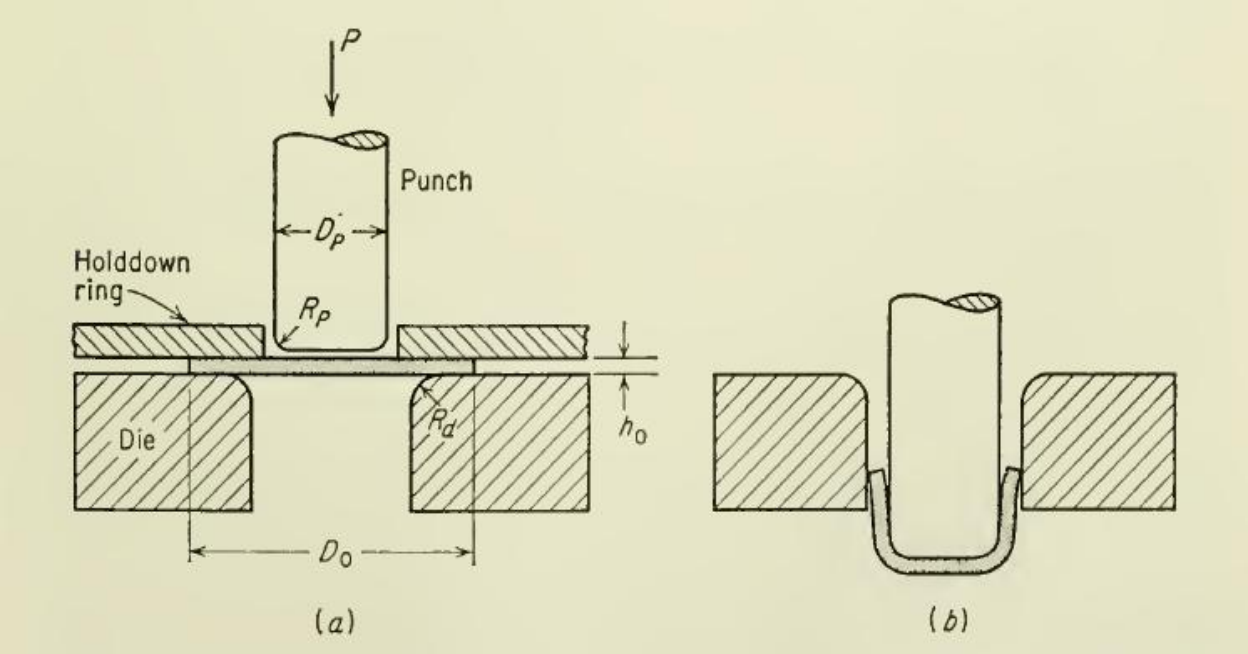

Fig. 3.1: Deep drawing of a cylindrical cup (a) Before drawing (b) After drawing [29]

Generally, a clamping or hold-down pressure is required to press the blank against the die to prevent wrinkling. This is best done by means of a blank holder or hold-down ring in a double-action press. The important variables in deep drawing are the properties of the sheet metal, the blank diameter, D_O; the punch diameter, D_P; the clearance, c, between punch and

die; the punch radius, R_P; the die-corner radius, R_d; the blank holder force, F_h; and friction and lubrication between all contacting surfaces.

3.2 Stages in Deep Drawing

The whole deep drawing process can be divided into 5 stages which are depicted as follows:

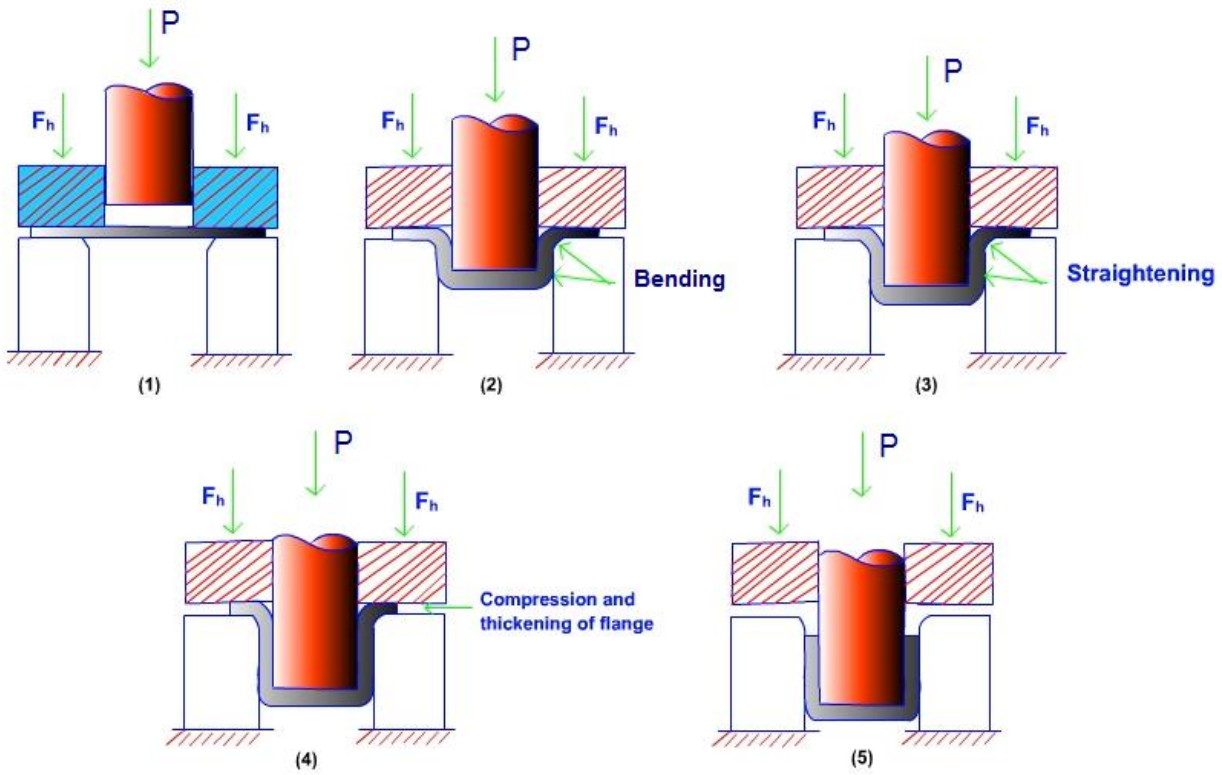

Fig. 3.2: Sequence of stages in deep drawing operation

1. Punch makes initial contact with blank
2. Bending
3. Straightening
4. Friction and compression
5. Final cup shape showing effects of thinning in the cup walls

The punch on coming in contact with the blank pushes the sheet into the die cavity. The flat portion of the sheet under the holding plate moves towards the die axis, then bends over the die profile. After bending over the die profile the sheet unbends to flow downward along

the side wall. The vertical portion of the sheet then slips past the die surface. More metal is drawn towards the center of the die in order to replace the metal that has already flown into the die wall. Friction between holding plate and blank and that between die and blank has to be overcome by the blank during its horizontal flow.

The metal taken from the flange of the shell is used up to produce increase in height of the part. A rather crude demonstration of this shift is depicted in Fig.3.3. Here the segments of material are being displaced, flowing away from the flange toward the body of the shell, pulled by the action of the drawing punch and drawing die.

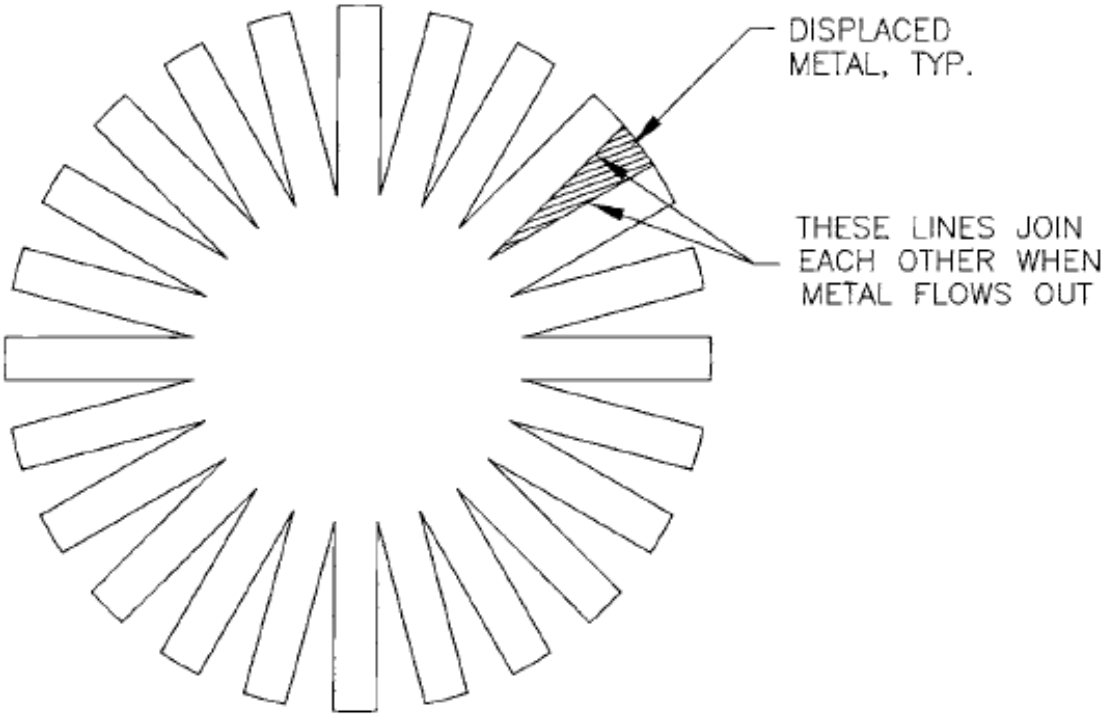

Fig. 3.3: Displacement of metal in drawing [30]

3.3 Stresses in Deep Drawing

On the basis of state of stress, the deep drawn cup can be divided into three regions, namely, the flange region, the cup wall and the punch region.

- **Flange:** It undergoes compressive hoop stress, radial tensile stress and compressive stress. The compressive hoop stress is induced due to the sheet being drawn towards the center. The

compressive hoop stress is due to the metal being drawn towards the center. The compressive stress due to the blank holder plate acts in the axial direction.

- **Cup Wall:** It is subjected to longitudinal and hoop tensile stresses.

- **Punch Region:** This area of the blank is subjected to biaxial tensile stress due to the punch action.

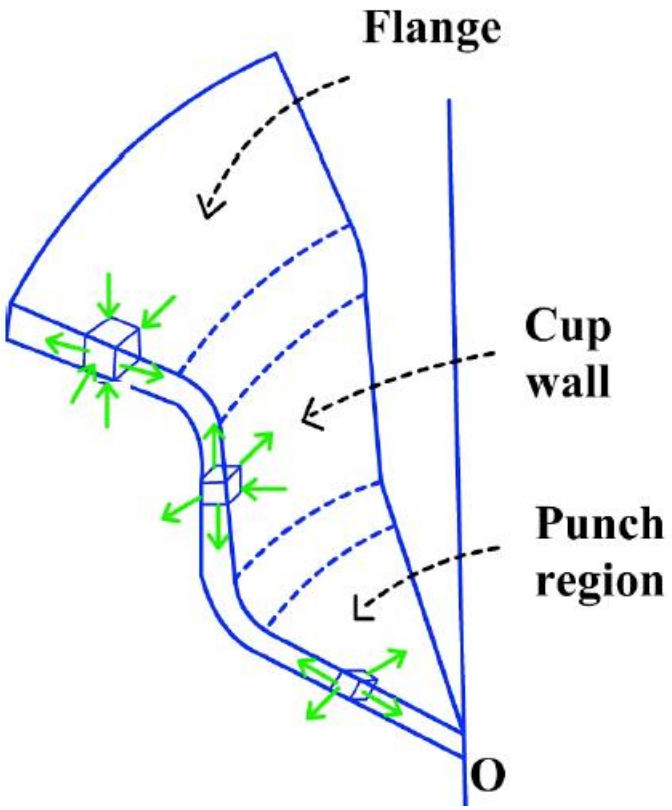

Fig. 3.4: Stresses in Deep Drawing

3.4 Deformations in Deep Drawing

In a typical deep drawing of a round cup, various deformation zones can be identified as given follows and also shown in the figure:

- Zone A-C: the flange (axial compression, radial tension, circumferential compression)
- Zone D-E: the die corner radius (bending and friction)
- Zone D-E: the wall of the cup (tension and potential fracture)
- Zone E-F: the punch corner radius (bending and friction)

- Zone F-G: the flat circular bottom (friction and near zero strain)

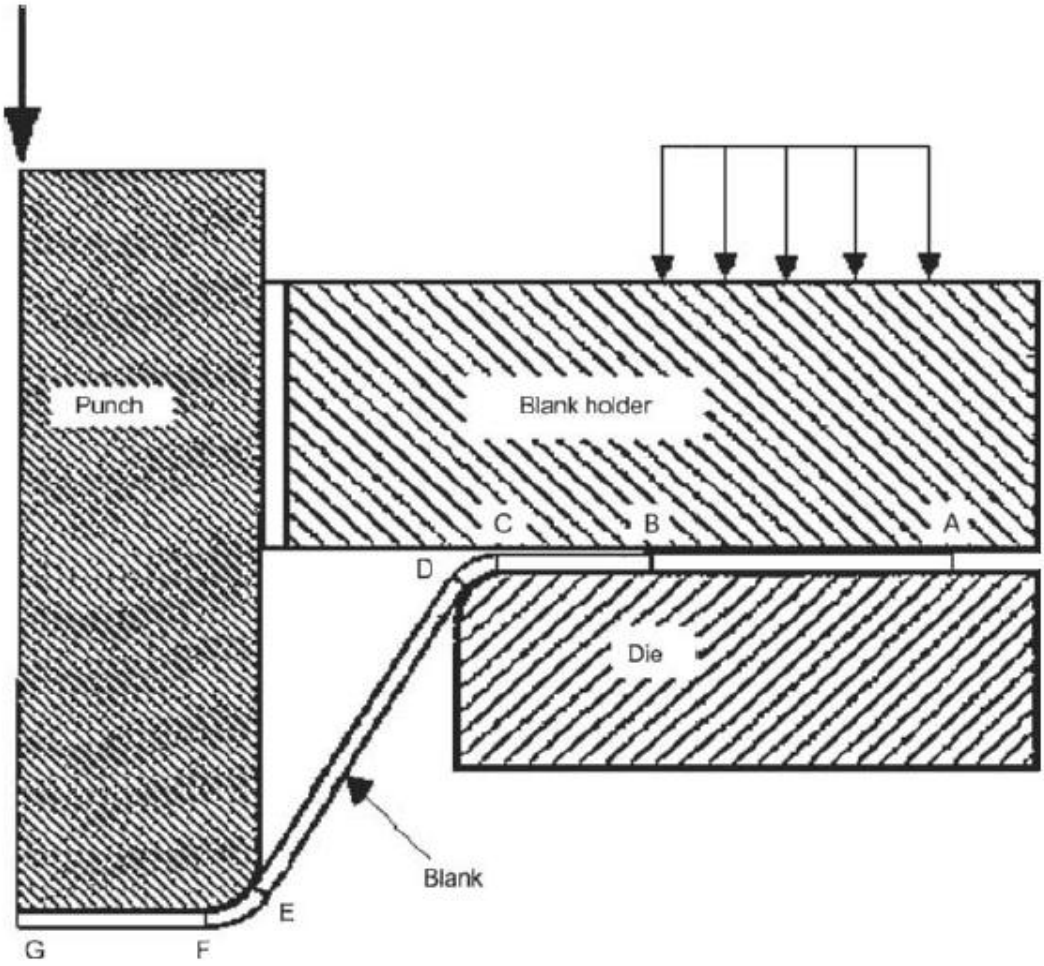

Fig. 3.5: Various deformation zones in deep drawing [31]

A detailed explanation is as follows:

Zone A-C: The majority of deformation occurs in the flange of the cup, which undergoes radial elongation and circumferential compression. As the punch draws the sheet into the die cavity, the perimeter of the sheet is forced into a smaller diameter, resulting in flange thickening (zone A-B). Also, because of drawing by the punch, the sheet material close to the die corner undergoes some reduction in thickness (zone B-C). As a result, k s portion of the flange may not contact the blank holder surface entirely.

Zone C-D: Once the material overcomes the compression of drawing through the flange, it must bend and unbend over the die radius. The state of stress in this zone is that of radial

elongation and bending over the die radius. If the radius is too small, the sheet may fracture at this location. If it is too large, then the draw depth is reduced and the formability of the material is not fully utilized. Hence, certain guidelines are established for the proper selection of the die radius.

Zone D-E: The state of stress in this zone is that of radial and circumferential tension. If the punch die clearance is large, the unsupported regions of the cup wall may experience a form of undergo out-of-plane deformation (similar to wrinkling) called puckering. The punch force is transmitted from the bottom of the cup to the deformation zone (flange) through tension on the wall of the cup. The tension must not cause the wall to deform plastically; otherwise, fracture may occur.

Zone E-F: In this zone, the sheet material undergoes bending over the punch corner radius and the state of stress is again that of radial tension. As the material bends over the die radius, it undergoes strain hardening. Hence, the flowing material, which forms the cup wall, becomes strengthened. The material at the punch corner radius is the most common failure site: the cup wall is weakest here because the portion of the sheet in this region has the least strain hardening.

Zone F-C: In this region, because of greater friction between the punch surface and the bottom of the cup, the material does not undergo much plastic deformation.

3.5 Drawability of Sheet Metals

3.5.1 Limiting Drawing Ratio

Drawing drawability can be defined as the capability of the sheet metal to be drawn successfully from the flange into die cavity using a punch with a particular diameter. The magnitude of the deformation of a deep drawn part is usually characterized by a drawing ratio β, which is defined as the ratio of the initial blank diameter D_0 to the inside diameter of the finished cup D_P .The larger the chosen drawing ratio, the larger will be the drawing load under otherwise constant conditions. This load must be transmitted by the wall of the deep drawn part. Therefore, the drawing ratio must not exceed a maximum value, limiting drawing ratio in order to prevent cracks at the bottom of the cup. This Limiting Drawing Ratio β_{max} is defined as the ratio of the maximum diameter of the circular blank to the diameter of the used punch, which can be attained without failure.

$LDR = (D_o/D_p)_{max} = e^{\eta}$

where η is the efficiency of drawing.

The maximum LDR for efficiency =100% is equal to 2.7.

If we assume an efficiency of 70% the maximum LDR is about 2. That means the maximum reduction possible in single deep drawing step is 50%. This is the general criteria for first draws.

3.5.2 Redrawing

Redrawing is reduction in diameter and increase in length of a cup which has been drawn to a certain draw ratio. In case of materials which are difficult to draw in one step, redrawing is performed. Generally, during the first stage upto 40% reduction is achieved. In the first redrawing after drawing, maximum of 30% reduction can be set. In the second redrawing stage, 16% reduction is set. In direct redrawing process, the angle of bending undergone by the cup is less than 90o, thereby reducing the draw force. In reverse redrawing, the outside surface of the drawn cup becomes the inner surface during redrawing. Wrinkling is controlled to a good extent in this process. Friction is higher in redrawing. Therefore larger reductions cannot be affected in redrawing.

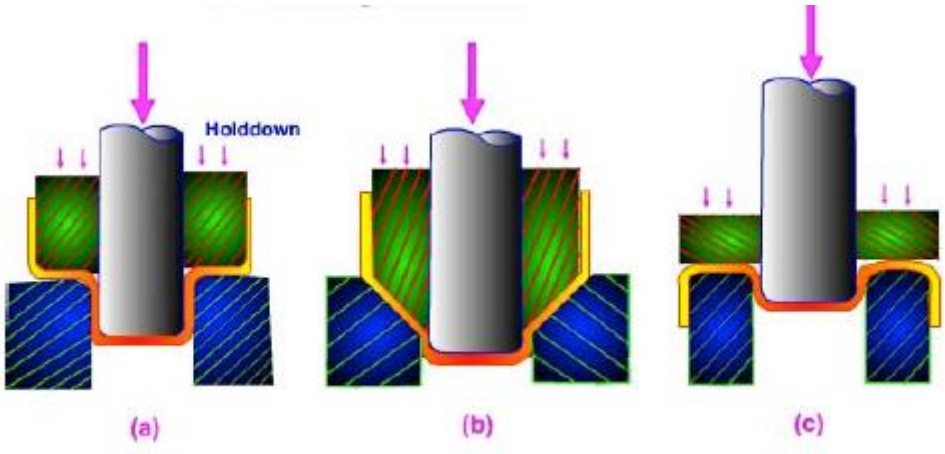

Fig. 3.6: Redrawing Methods (a) Direct redrawing (b) Direct redrawing with tapered die (c) Reverse redrawing

3.6 Formability of Sheet Metals

Formability is a term applicable to sheet metal forming. Sheet metal operations such as deep drawing, cup drawing, bending etc involve extensive tensile deformation. Therefore, the problems of localized deformation called necking and fracture due to thinning down are common in many sheet forming operations. Anisotropy also is a major concern in sheet metal operations. Formability is the ease with which a sheet metal could be formed into the required shape without undergoing localized necking or thinning or fracture. When a sheet metal is subjected to plane strain deformation, the critical strain, namely, the strain at which localized necking or plastic instability occurs can be proved to be equal to 2n, where n is the strain hardening exponent. For uniaxial tensile loading of a circular rod, the critical or necking strain is given to be equal to n. Therefore, if the values of n are larger, the necking strain is larger, indicating that necking is delayed. In some materials diffuse necking could also happen. Simple uniaxial tensile test is of limited use when we deal with formability of sheet metals. This is due to the biaxial or triaxial nature of stress acting on the sheet metal during forming operations. Therefore, specific formability tests have been developed, appropriate for sheet metals.

3.6.1 Formability Tests

Some of the widely used formability tests have been described below:

3.6.1.1 Erichsen Test

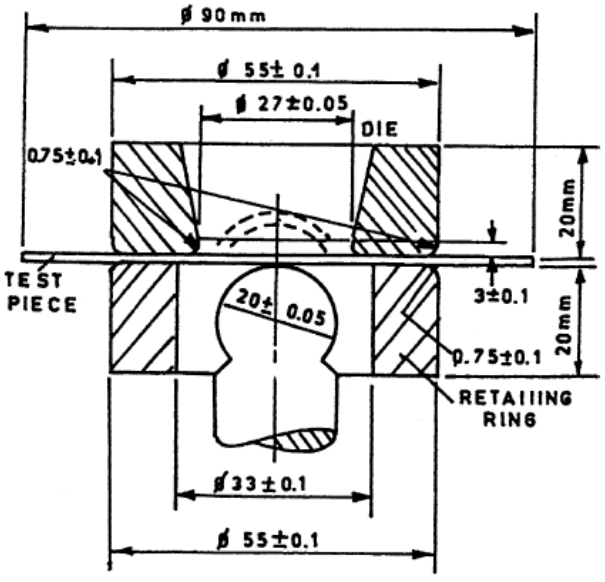

Fig. 3.7: Scheme of Erichsen Test [32]

The test consists of stretching a sheet specimen by means of a hemispherical punch until the occurrence of fracture. The depth of the punch indentation in the specimen expressed in millimeters is the Erichsen index (IE). This is the most commonly used parameter for expressing the formability of sheet metals.

3.6.1.2 Swift's Cup Test

This test consists of deep-drawing cylindrical parts having different diameters and determining the limit drawing ratio LDR. Swift's method has been widely used and is considered as a standard test by the International Deep-Drawing Research Group (IDDRG) [33,34].

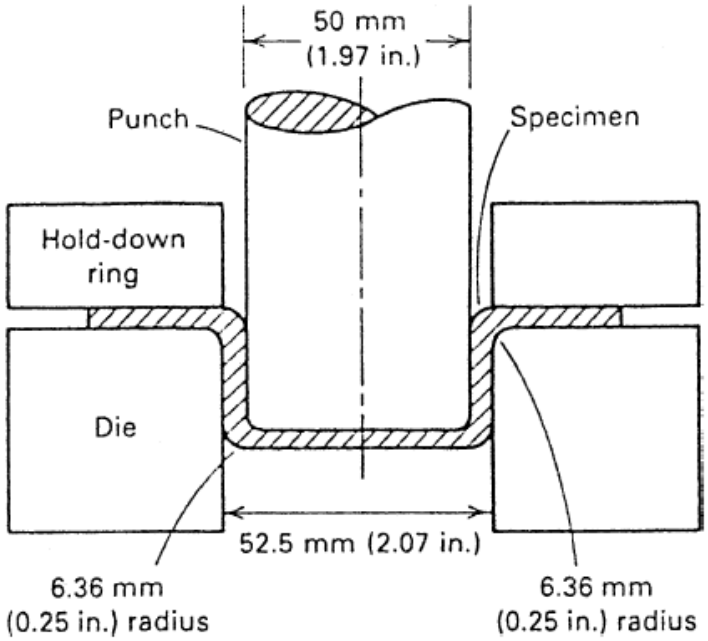

Fig. 3.8: Scheme of Swift's Cup Test [35]

3.6.1.3 Fukui Test

Fukui proposed a deep drawing test using a conical die. The advantage of this method is that the 'diameter ratio' $D/D0$ (D = upper diameter of the part at fracture) as a measure of formability may be established by a single test.

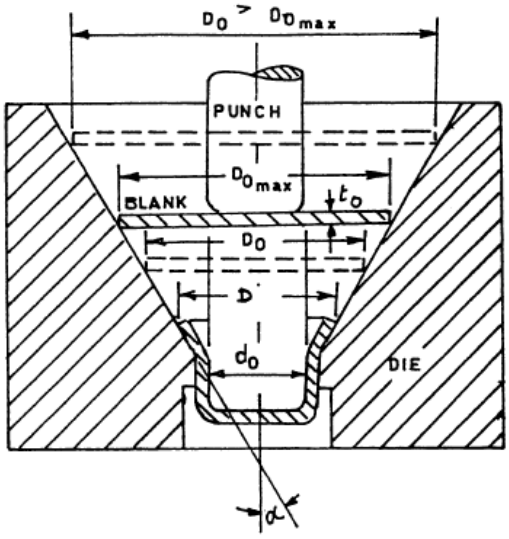

Fig. 3.9: Scheme of Fukui Test [36]

3.6.2 Forming limit diagram (FLD)

Forming limit diagram is a very effective way of optimizing sheet metal forming. A grid of circles is etched on the surface of a sheet metal. Then the sheet metal is subjected to deformation. Usually the sheet is deformed by stretching it over a dome shaped die. Strips of different widths can be taken for the test, in order to induce uniaxial or biaxial stress state. The circles deform into elliptic shapes. The strain along two principal directions could be expressed as the percentage change in length of the major and minor axes. The strains as measured near necks or fracture are the strains for failure. A plot of the major strain versus minor strain is then made. This plot is called Keeler-Goodwin forming limit diagram. This plot gives the limiting strains corresponding to safe deformations. The FLD is generally a plot of the combinations of major and minor strains which lead to fracture. Combination of strains represented above the limiting curves in the Keeler-Goodwin diagram represent failure, while those below the curves represent safe deformations.

A typical Keeler-Goodwin diagram is shown below. The safe zone in which no failure is expected is shown as shaded region. Outside this zone there are different modes of failure represented at different combinations of strains. The part above the safe zone represents necking and fracture. The slope of the right hand side curve (necking curve) is found to decrease with increasing values of the strain hardening exponent, n. Similarly, variations in sheet thickness, composition, grain size all reduce the slope of the neck curve. The safe

region is narrowed down by biaxial stress state. Sheet thickness also has effect on FLD. Higher sheet thickness increases the FLD.

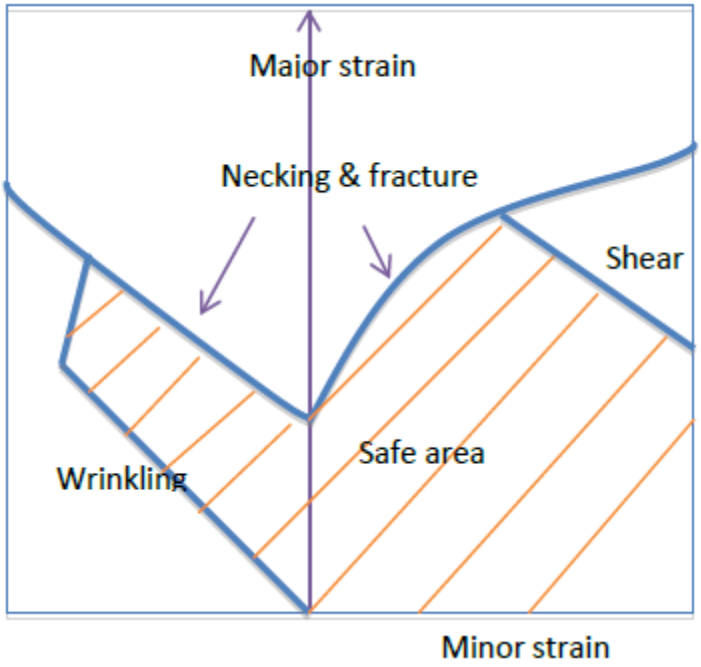

Fig. 3.10: Keeler-Goodwin diagram

3.7 Parameters affecting Deep Drawing

Since the deep drawing process is employed for manufacturing of products of various shapes and sizes, and from different materials, a thorough understanding of the factors affecting the process is important, from both engineering and economic viewpoints. These parameters can be classified into three categories**: material**, **geometric** and **process** parameters.

3.7.1 Material Parameters

These include strength coefficient K, strain hardening coefficient n and anisotropy.

3.7.1.1 Strength Coefficient, K

A high **K**-value means a strong wall, which is beneficial, but also a strong flange, which makes it harder to draw in. Therefore, for the drawing operation to be successful, the **K**-value should be sufficiently large to assure a product of reasonable strength, but not so high such that it necessitates use of large punch force to complete the draw, which in turn might cause fractures.

3.7.1.2 Strain-hardening exponent

The strain-hardening exponent, ***n,*** is an indicator of material formability and plays a crucial role in sheet metal forming. A higher **n**-value strengthens the cup wall, but it also strengthens the flange so that more force is needed to deform it. Nevertheless, the LDR tends to increase with increasing n-value.

3.7.1.3: Anisotropy

An average or normal plastic anisotropy,$\bar{r}$**,** is calculated as:

$$\bar{r} = \frac{r_0 + 2\,r_{45} + r_{90}}{4}$$

where r_0,r_{45} and r_{90} are r-values at 0°, 45° and 90° from the rolling direction.

Increasing r-values decrease the force required to deform the flange while increasing the strength of the cup wall. The r-value indicates the ability of the material to resist thinning. When r>1, the material flows easily in the plane of the sheet but not in the thickness direction. On the other hand, r<1 means that the material flows easily in the thickness direction, and this is an undesirable property as it might lead to excessive thinning.

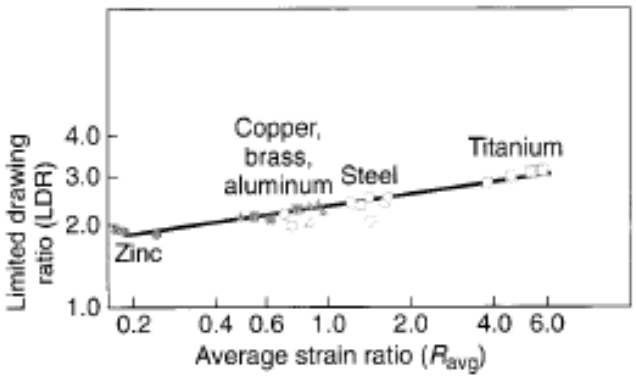

Fig. 3.11: The relationship between average normal anisotropy and the limiting drawing ratio for various sheet metals. [4]

For an anisotropic material, drawability will be given by

$$\ln(\mathrm{LDR}) = \sqrt{(r+1)/2}$$

Planar anisotropy, Δr, is calculated as:

$$\Delta \mathbf{r} = \frac{\mathbf{r_0} - \mathbf{2r_{45}} + \mathbf{r_{90}}}{\mathbf{2}}$$

The higher the values of Δr, the more earing occurs. Earing typically must be trimmed; therefore, an increase in Δr increases trimming and reduces the total depth of draw.

3.7.2 Geometric Parameters

Punch and die geometry influence metal flow and friction in deep drawing.

3.7.2.1 Die Radius

Too small a die radius leads to fracture as material does not flow smoothly over small the die radius. Therefore, large die radius is preferred for decreasing the drawing load and increasing the LDR. However, the contact area between the blank holder and the flange becomes smaller with increasing die radius, which may result in wrinkles in the die radius region. The recommended die radii for first and subsequent redraws are (6 to 10)t and (6 to 8)t respectively, where t is the initial blank thickness.[36]

3.7.2.2 Punch Radius

Fracture normally occurs at the bottom or the heel of the cup wall (where the punch radius meets the cup wall). This is the weakest point in the cup because it does not undergo as much work hardening as do the sides of the wall. The walls are strengthened by work hardening due to bending and unbending of the sheet over the die radius. As the punch corner radius is increased, the failure site moves upwards into the material (cup walls) that has been strengthened by prior work hardening. A generous corner radius also results in a gradual increase of the punch load with stroke.

Punch radii values differ with the diameter of shell d as follows: [30]
For d= 0.25 to 4.0 in. [6.3 to 100 mm], R_P = (3 to 4)t
For d= 4.0 to 8.0 in. [100 to 200 mm], R_P = (4 to 5)t
For d= above 8.0 in. [200 mm], R_P = (5 to 7)t

3.7.2.3 Punch-Die Clearance

If the clearance between the die and the punch is smaller than the thickness of the upper portion of the cup, this portion's thickness will be reduced due to ironing. During the ironing process, the gap between the die and the punch is larger than the initial blank thickness but smaller than the expected thickness at the top of the cup. As a result, the top of the cup (where the cup is thickened the most) is squeezed between the die and the punch, and a cup with more uniform wall thickness is produced. This ironing process requires a considerable punch force, and if the cup is nearly formed before ironing occurs, the punch load/punch stroke diagram exhibits a second maximum (see Fig. 3.12).

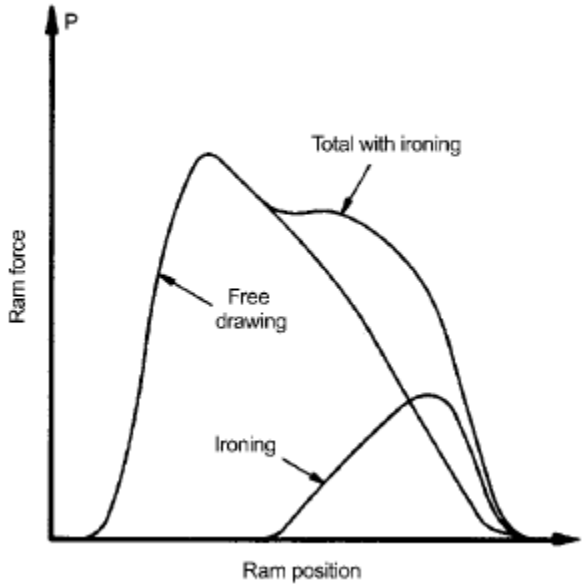

Fig. 3.12: Punch force/punch stroke diagram: ironing process combined with forming.[31]

3.7.3 Process Parameters

3.7.3.1 Lubrication

During a deep drawing process, friction exists at three interfaces:

- Between the blank holder and the flange
- Between the flange and the die
- Between the blank and the punch

Low friction at the die/blank holder interface and high friction at the punch and cup interface lead to larger achievable LDRs. Values for coefficients of friction in deep drawing are typically in the range of 0.04 to 0.10.Therefore, according to the shape and geometry of the drawn shell required, proper lubrication should be done such that these coefficients of friction can be used as controlling factors to control the metal flow from flange to cup region, wrinkling effect and percentage thinning.

3.7.3.2 Punch Velocity

Punch speed affects friction at the blank-punch interface. As a result, it may determine whether the wall of a drawn part will rupture, particularly at the moment when drawing begins. Punch speed should be adjusted according to the complexity of the die geometry and the performance of the lubricant. Such adjustment is possible in hydraulic and servo-drive presses that allow the adjustment of the punch speed during the stroke. In mechanical presses, various link drives are used to achieve high approach, low impact, low deformation, and high return speeds of the punch.

Material	Drawing Speed(mm/sec)
Steel	91-254
Stainless Steel	152-203
Copper	635-762
Zinc	635-762
Aluminum	762-889
Brass	889-1016

Table 3.1: Typical drawing speeds for various materials [31]

3.7.3.3 Blank Holder Force

The blank holder force (BHF) is applied to prevent wrinkling in the flange as well as in the wall of the drawn cup. Excessive BHF leads to fracture in the cup wall (Fig.). The maximum draw depth corresponds to simultaneous failure by wrinkling and failure. For any depth of cup less than the corresponding BHF value, there is a "window" of allowable BHF (Fig.). The BHF necessary to avoid wrinkling depends on the drawing ratio, sheet material and the relative blank thickness. As the relative blank thickness (s_0/d_0) decreases, the tendency to wrinkle increases, which necessitates more BHF to control the flow and prevent wrinkling. The blank holder pressure required to prevent wrinkling of the sheet can be estimated as: [31]

$$p_{BH} = 10^{-3}\, c \left[(DR - 1)^3 + \frac{0.005 d_0}{s_0}\right] S_u$$

$$F_{BH} = p_{BH} \text{ X } A_{BH}$$

p_{BH} is the blank holder pressure

F_{BH} is the blank holding force

A_{BH} is the area of the blank holder

c is the empirical factor, ranging from 2 to 3

DR is the drawing ratio

d_0 is the blank diameter

s_0 is the blank thickness

S_u is the ultimate tensile strength of the sheet material

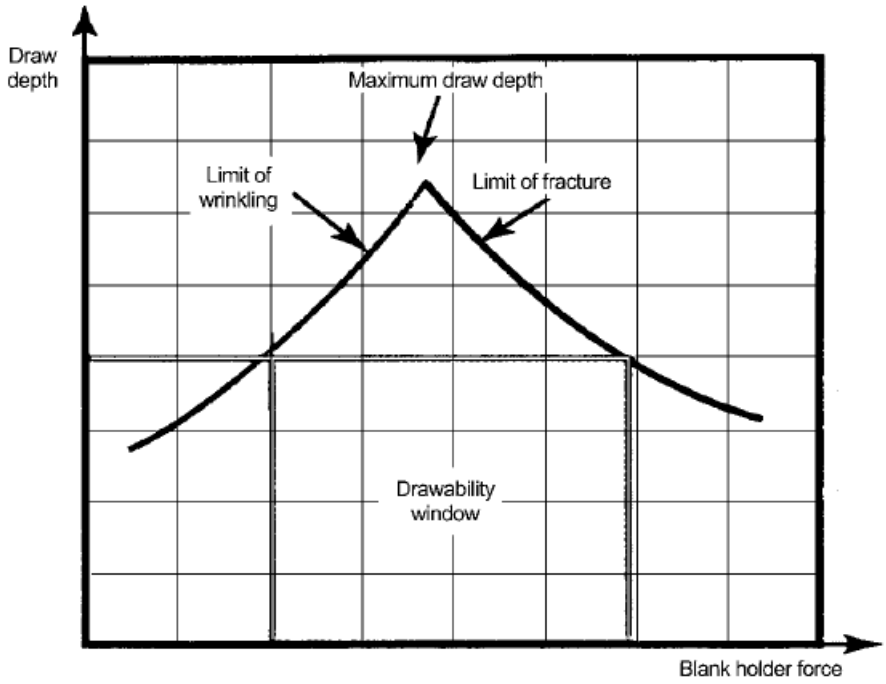

Fig. 3.13: Relationship between allowable blank holder force and draw depth [31]

3.8 Defects in Deep Drawing

As discussed in the previous section, the process of deep drawing is influenced by various factors, and when these parameters are not maintained during the process, a deep drawn part is susceptible to one or more defects. Major failure types that can be seen in a deep drawing process are wrinkling, necking, tearing, earing and poor surface appearance, as seen in figure.

Tearing and necking are tensile instability caused by strain localization. This reduces the strength of the part and the appearance worsens because of tearing and necking. It may be caused due to too small radii of the punch or die. Shells also tend to break at the heel area (punch radius area) if the drawing reduction ratio for a single pass is too large. Radial cracks may also occur in the flange or the edge of the cup, indicating that the metal lacks sufficient ductility to withstand the large amount of circumferential shrinking that is required in this region of the blank.

Wrinkling of the flange or the edges of the cup is the result of buckling of the sheet as a result of the high circumferential compressive stresses. In analyzing this type of failure each element in

the sheet can be considered as a column loaded in compression. Since column stability decreases with an increasing slenderness ratio, the critical buckling load will be achieved at lower loads for thin sheet. If the punch load is high and exceeds the critical buckling load of the column, it leads to wrinkling.

Earing refers to the wavy edges on the top of a deep drawn cup. The number of ears may be two, four, six or even eight, but the most common are four ears. Earing is the inevitable result of planar anisotropic behaviour of the sheet material. Therefore, allowance for trimming the wavy edge area should be taken into consideration when calculating blank size.

Ring prints, traces, orange skin (or orange peel structure), and Lüders strips are the surface appearance defects. Those regions of the part which have undergone appreciable deformation exhibit pronounced surface roughness are usually known as orange peels. This effect occurs in sheet metal of relatively large grain size. It results from the fact that the individual grains tend to deform independently of each other, and therefore the grains stand out in relief on the surface. Lüders strips or stretcher strains are a serious defect commonly found in low carbon steel sheet. It shows a flamelike pattern of depressions on the surface. These depressions first appear along planes of maximum shear stress, and then, as deformation continues, they spread and join together to produce a uniform rough surface.

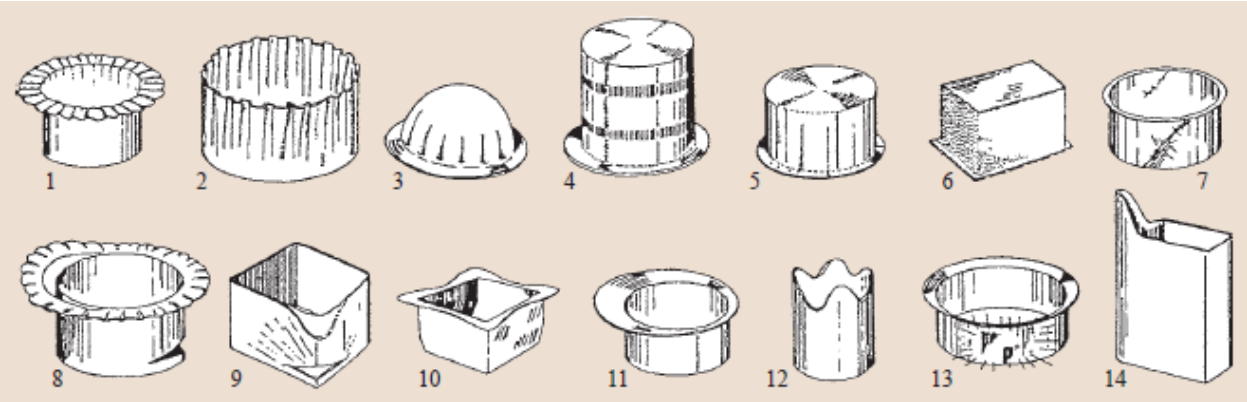

Fig. 3.14: Various failure modes in deep-drawing: 1-flange wrinkling; 2-wall wrinkling; 3- part wrinkling; 4-ring prints; 5- traces; 6-orange skin; 7-Lüder's strips; 8-bottom fracture; 9- corner fracture; 10,12-folding; 13,14-corner folding. [2]

CHAPTER 4

MODELING AND SIMULATION

4.1 Modeling

Modeling of the product has been done using SolidWorks 13.0 academic version. SolidWorks is a 3D solid modeling software used by students, designers, engineers, and other professionals to produce simple as well as complex parts, assemblies, and drawing. SolidWorks is beneficial because it saves time, effort, and money that would otherwise be spent prototyping the design.

4.1.1 Stage One

First stage die was designed after carrying out simulations for different depths and die radius, keeping in view the strain hardening phenomenon and thinning %. A drawing ratio of 2.45 was taken, owing to the taper in the die.

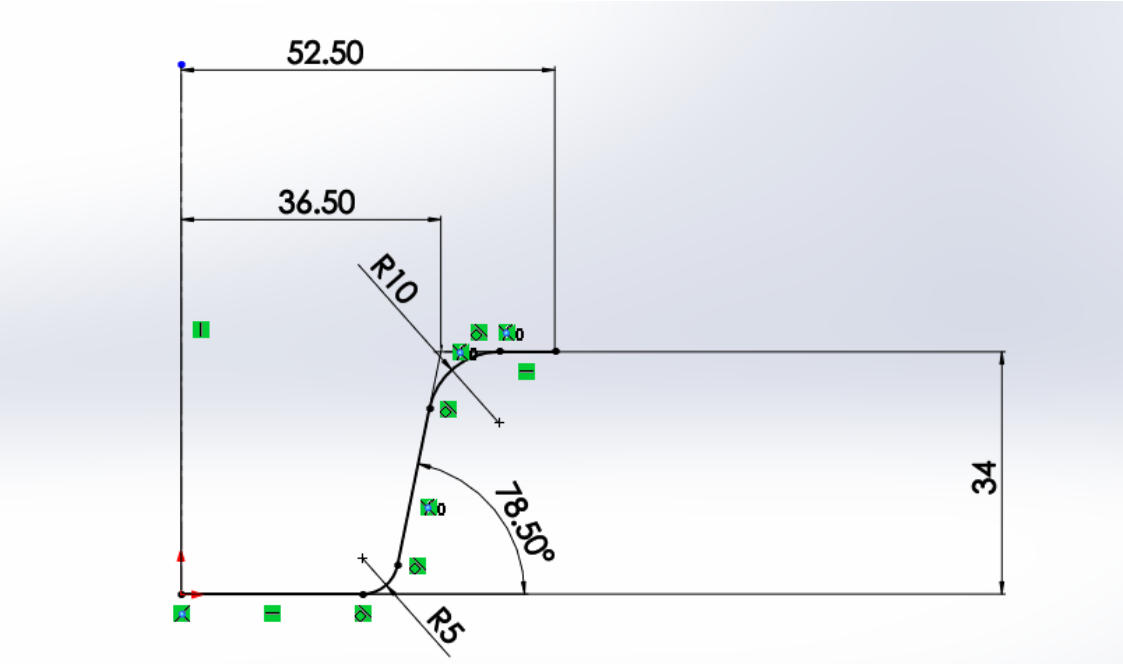

Fig. 4.1: 2-D drawing of first stage die

Fig. 4.2: 3-D model of first stage die

4.1.2 Stage Two

After the first stage, due to the strain hardening of the material, the product could be drawn further by only 8 mm.

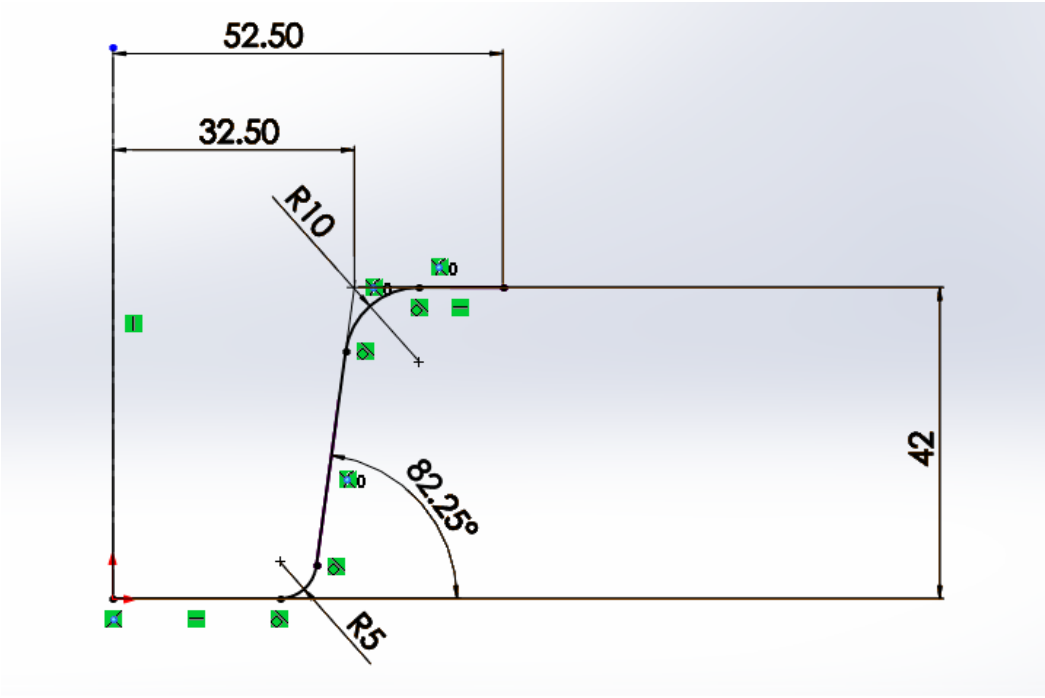

Fig. 4.3: 2-D drawing of second stage die

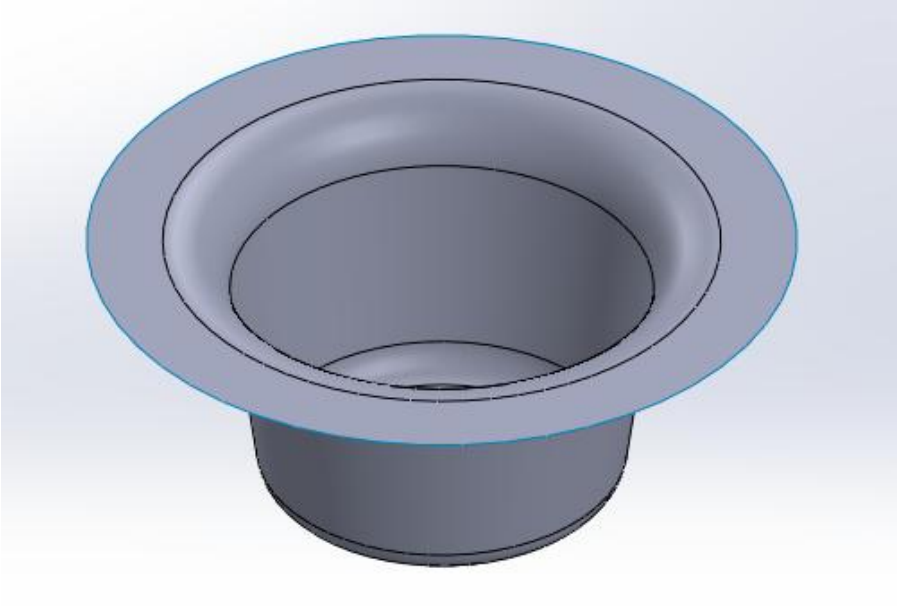

Fig. 4.4: 3-D model of second stage die

4.1.3 Stage Three

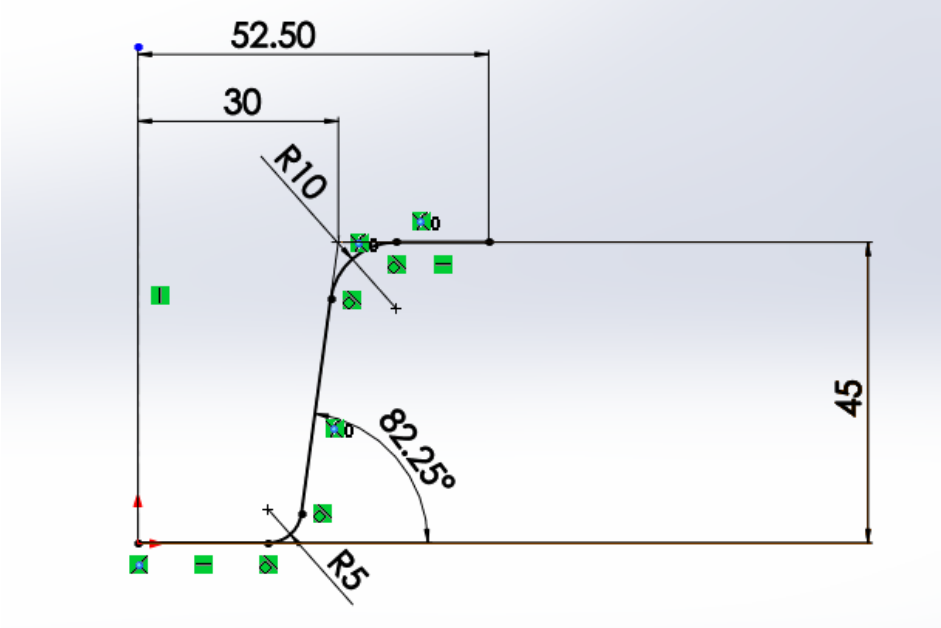

Fig. 4.5: 2-D drawing of the component

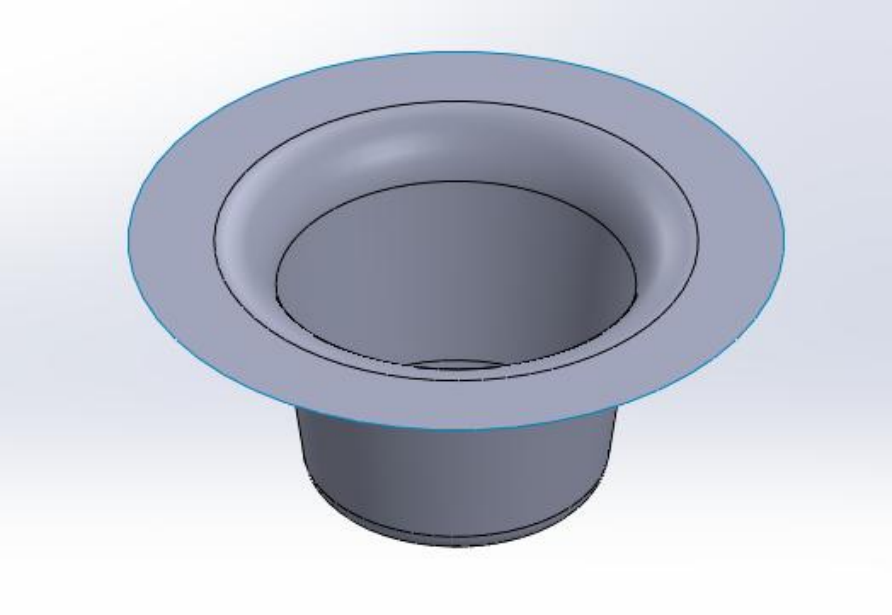

Fig. 4.6: 3-D model of the component

4.2 Simulation

Simulation is done using Altair Hyperform Radioss which is a comprehensive finite-element-based sheet metal forming simulation framework. Its unique process-oriented environment captures the forming process with a suite of highly tailored and configurable analysis and simulation tools. HyperForm delivers a cost-effective solution that allows users to develop an optimal manufacturing process. Two modules of Hyperform Radioss are used, namely Radioss One-Step and Incremental Radioss.

One-Step is a designer friendly model setup for forming feasibility analysis. The solver is very fast and accurate in predicting the blank shape and forming feasibility early in the product development cycle, minimizing downstream formability challenges and associated costs. Its intuitive nesting interface proposes proper blank-sizing, minimizing material scrap in the early stages of the product development process.

Incremental is the module where actual forming simulation takes place. Here, we setup the deep drawing process, either manually through User Process or automatically through Auto

Process. It also has function known as Tool Setup that auto generates punch/die and blank holder meshes form the die/punch mesh using input data such as clearance percentage and blank holding area.

The results are viewed and processed in HyperView.

4.2.1 Radioss One-Step Analysis

In this analysis, CAD geometry, preferably in .igs format is imported and then processed before submitting for feasibility analysis. This processing includes removing holes, if any in the geometry, geometry cleanup, meshing with rigid mesh, autotipping with respect to the drawing direction, which is along z-axis by default, applying material properties, constraints and blank holding pressure.

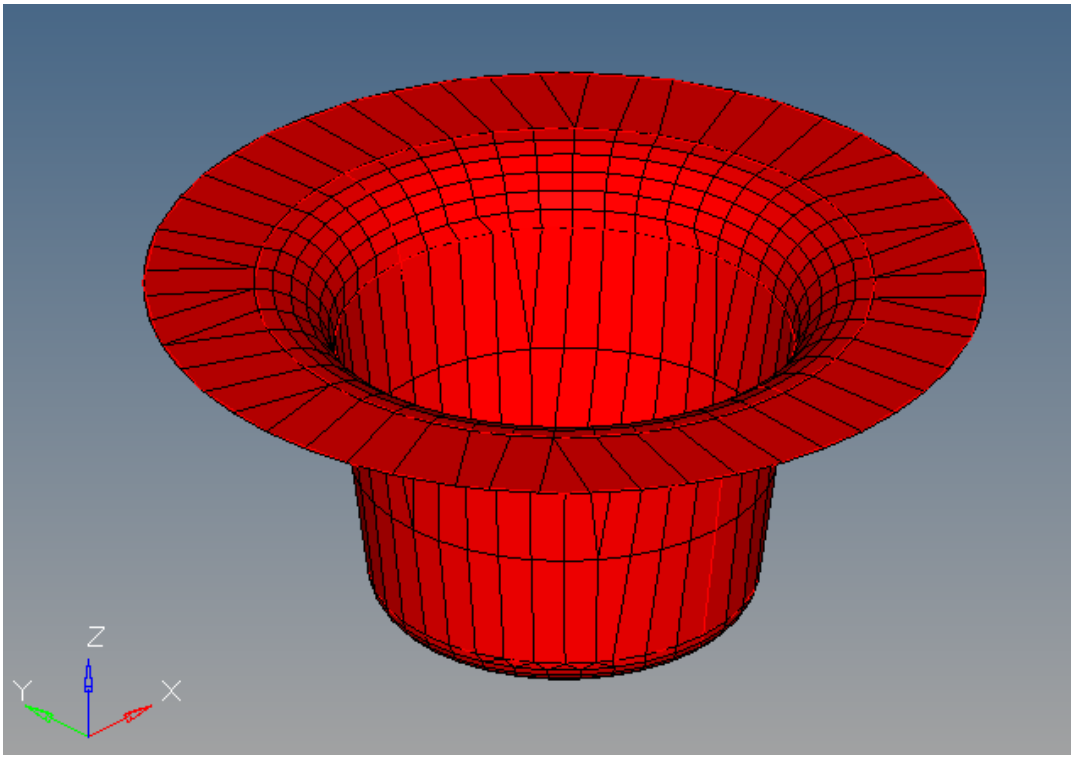

Fig. 4.7: Meshed geometry of the product to be drawn and aligned along z-axis

4.2.2 Incremental Radioss Analysis

4.2.2.1 Stage One

In this stage, we import the .igs file containing initial blank and die geometry. First, the die and blank are meshed and then Tool Setup function is used to build and setup the punch and binder from die surface. The Tool Setup function also automatically assigns meshes to punch and binder. The following figure shows the outcome of the Tool Setup function using die-punch clearance as 10%. Die, punch and binder are placed such that they just touch the blank surface.

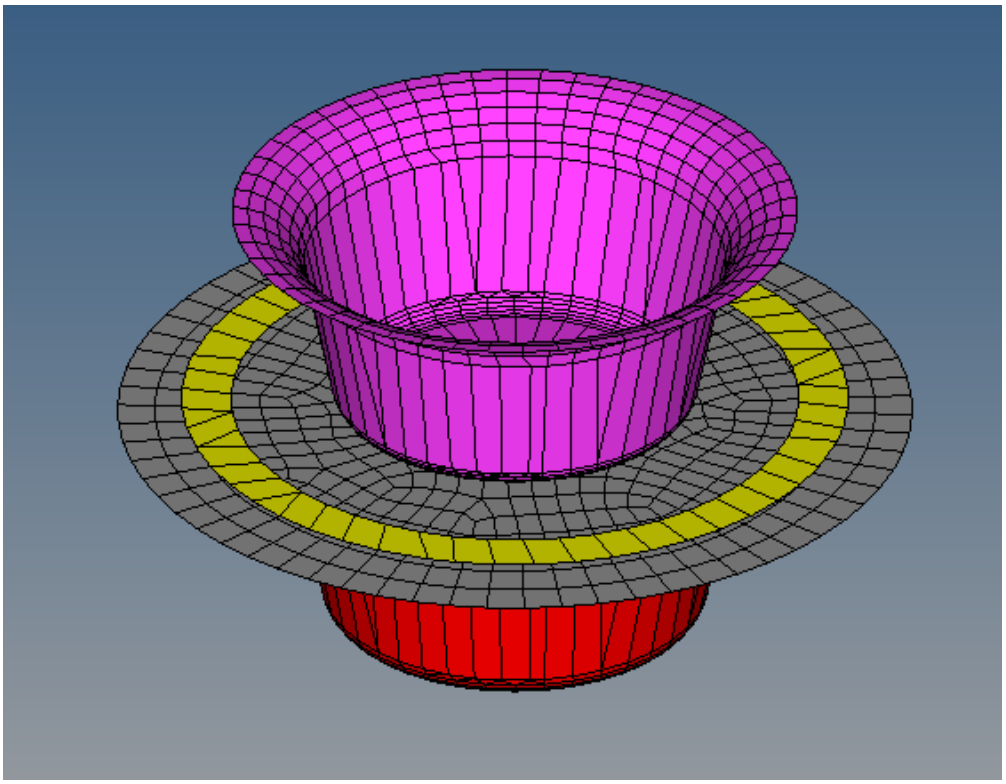

Fig. 4.8: Die, Blank, Binder and Punch after first stage Tool Setup

Die, punch and binder have been assigned rigid meshes known as R-Mesh consisting of four-node shell elements as they are tools and do not need to be analysed. Binder has been assigned fine B-Mesh or Belytschko-Tsay shells in order to capture the results with accuracy.

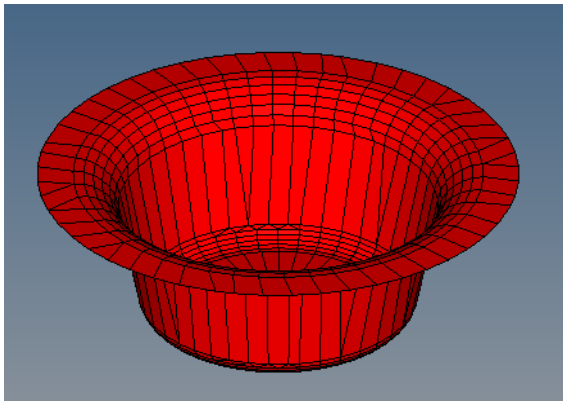

(a) Die

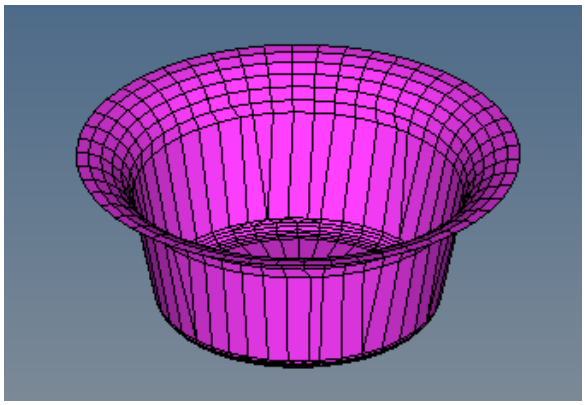

(b) Punch

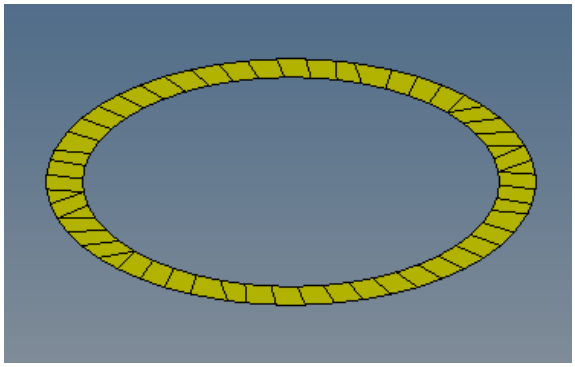

(c) Binder

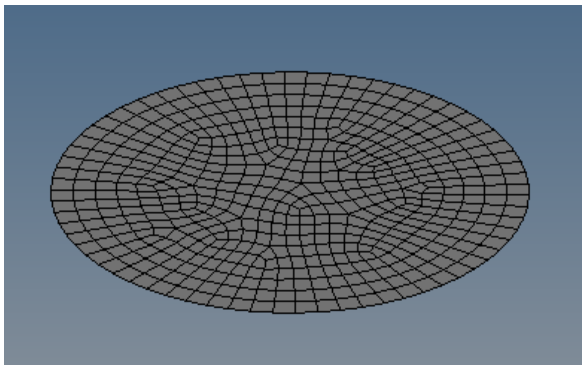

(d) Blank

Fig. 4.9: Meshes of (a) Die (b) Punch (c) Binder (d) Blank

After the Tool Setup, Auto Process is selected in order to finally setup the analysis. We set the material to be used for sheet as CRDQ (Cold Rolled Deep Quality).

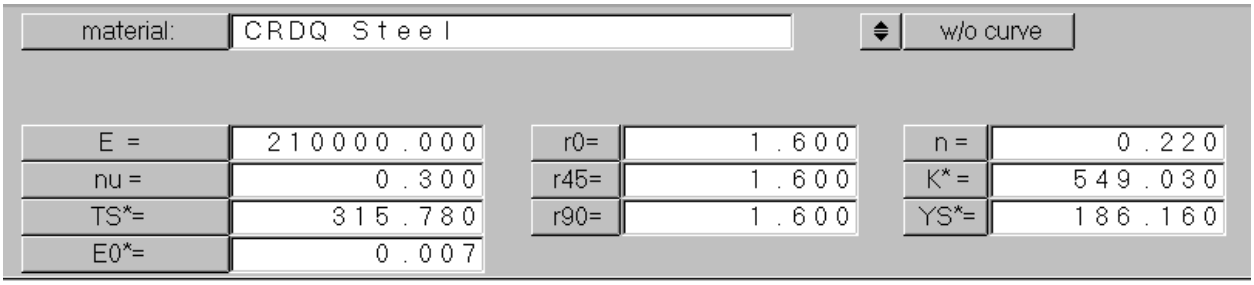

Fig. 4.10: Material Properties for CRDQ

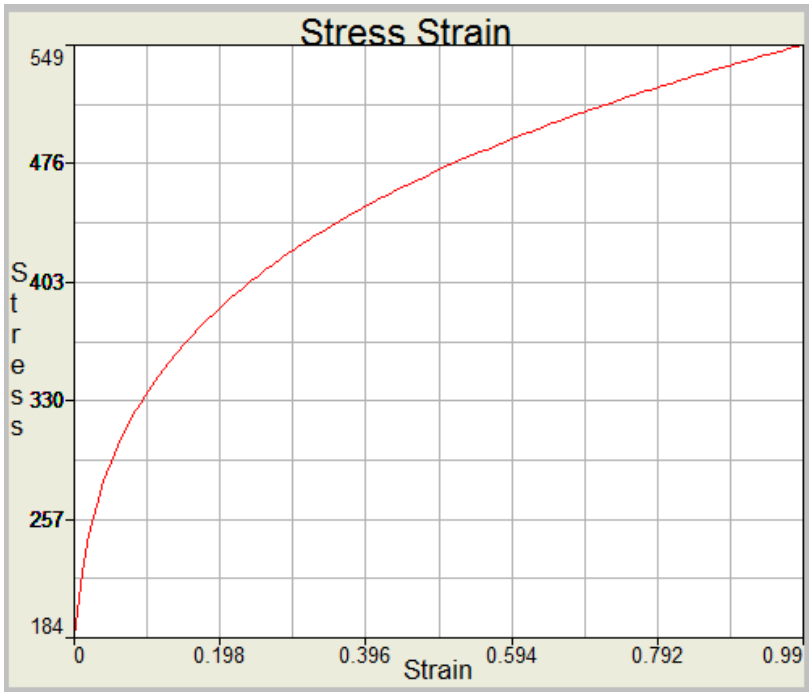

Fig. 4.11: Stress Strain curve for CRDQ

As this is a double action draw, travel and velocity details for punch are asked. When we click on Autoposition, these travel details are calculated by the software and automatically fed, with respect to the condition that all other tools just touch the blank. We can also change these values according to our requirements.

The frictional coefficients between various surfaces are as given below:

S.No.	Contact Surfaces	Coefficient of friction
1	Die-Blank	0.125
2	Binder-Blank	0.125
3	Punch-Blank	0.125

Table 4.1: Coefficients of friction for different contact regions

Then we click on Apply to apply these values to the model and Run to run the analysis using Radioss.

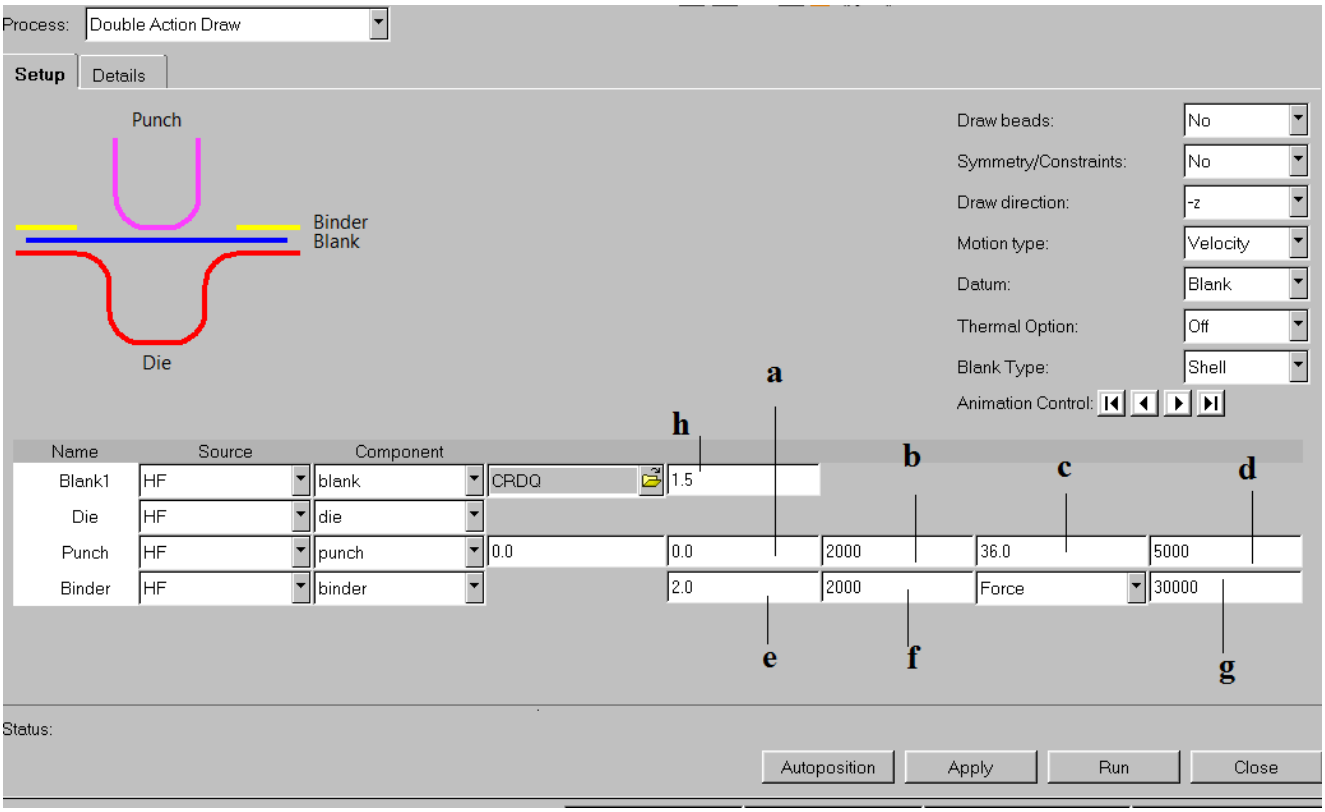

Fig. 4.12: First stage Auto Process window (a) Punch travel towards binder(mm) (b) Velocity of punch during its travel towards binder(mm/sec) (c) Punch travel towards die(mm) (d) Velocity of punch during its travel towards die(mm/sec) (e) Binder travel towards die(mm) (f) Velocity of binder travel towards die(mm/sec) (g) Blank Holding Force(Newtons) (h) Blank Thickness(mm)

4.2.2.2 Stage Two

In this stage we import .igs file containing the second stage die geometry and .sta file created after the first stage containing node and element definitions of the part formed after first stage, which is to serve as the blank for second stage. Hyperform automatically creates a .sta.hmx file while importing .sta file. This .sta.hmx file contains the adaptive constraints, initial stress and initial strain quantities.

We again mesh the die surface while the blank is already meshed, and use Tool Setup to again build and setup the punch and binder meshes.

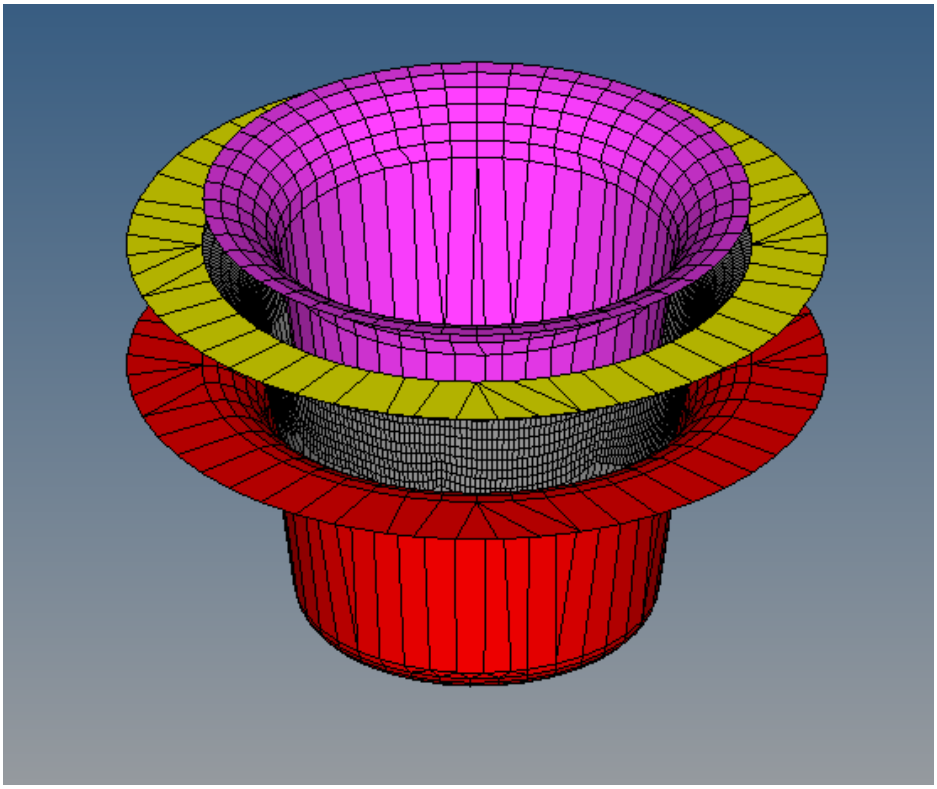

Fig. 4.13: Die, Blank, Binder and Punch after second stage Tool Setup

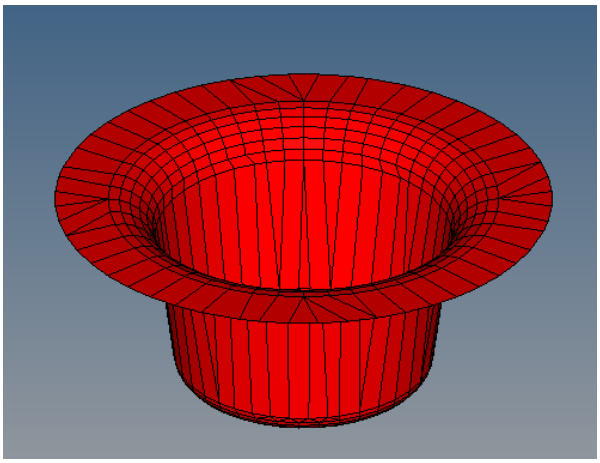

(a) Die

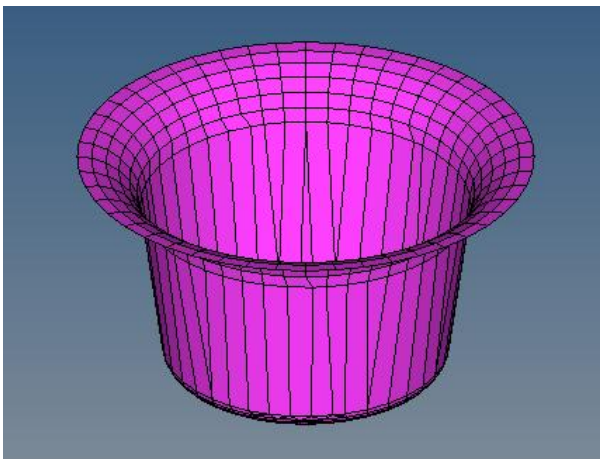

(b) Punch

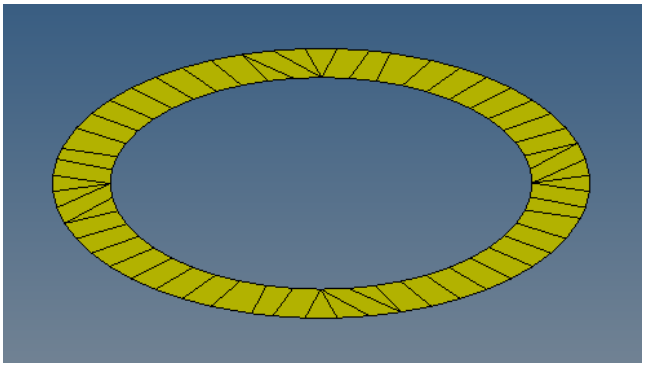

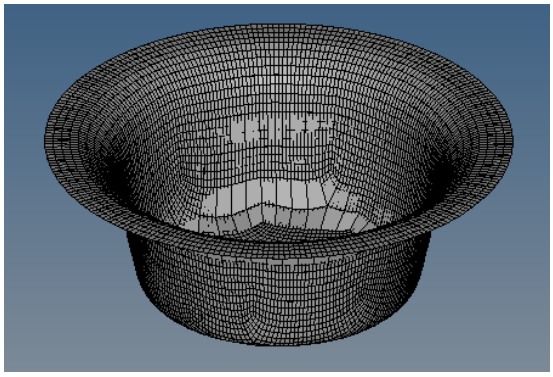

(c) Binder **(d) Blank**

Fig. 4.14: Meshes of (a) Die (b) Punch (c) Binder (d) Blank

The Autoprocess window is as follows:

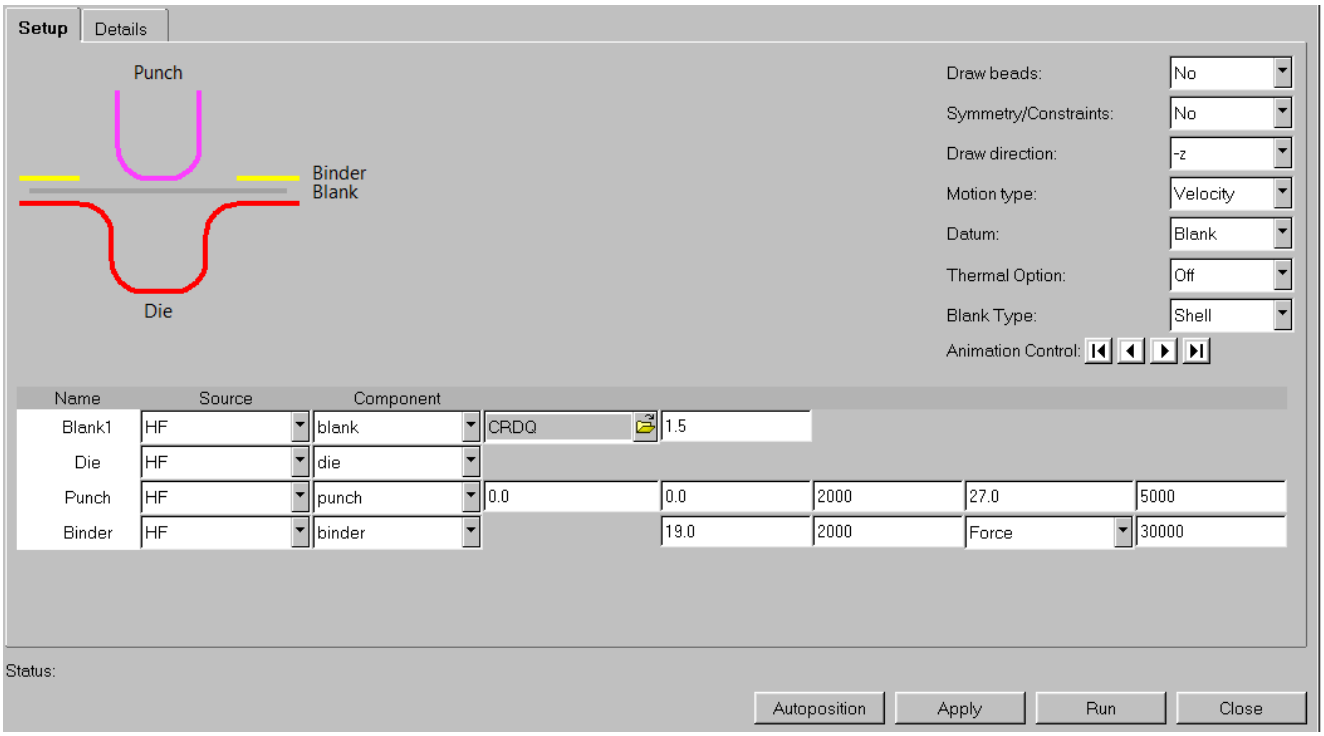

Fig. 4.15: Second stage Auto Process window

4.2.2.3 Stage Three

The same procedure is applied in this stage to import .sta and .igs files and setup the tools.

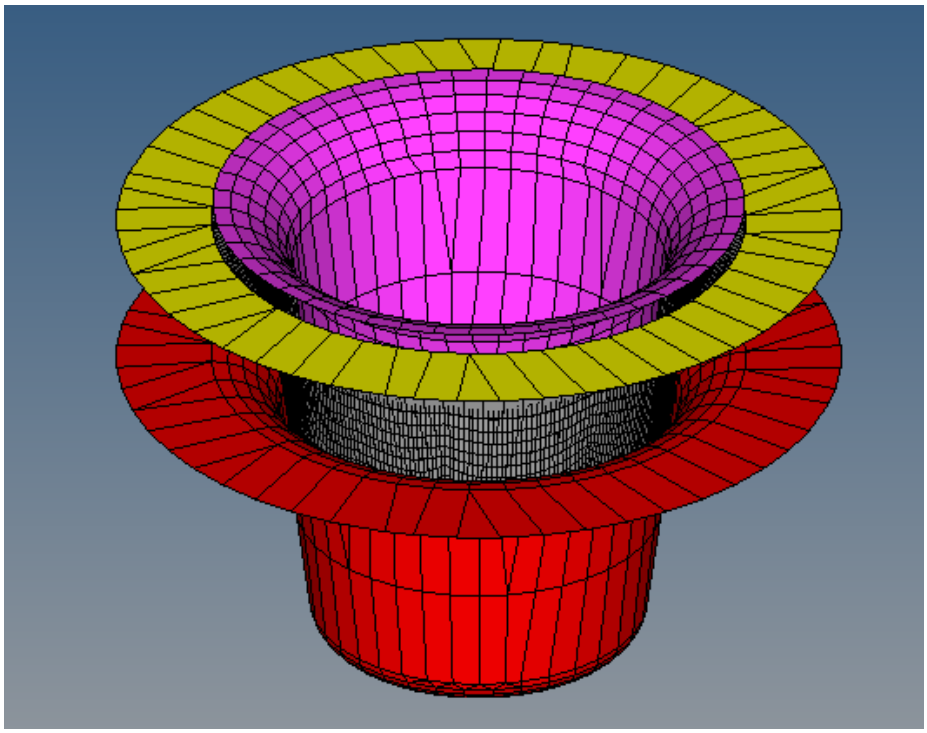

Fig. 4.16: Die, Blank, Binder and Punch after third stage Tool Setup

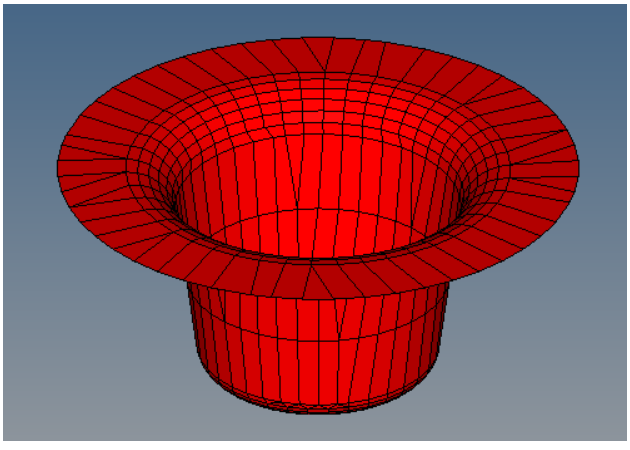

(a) Die

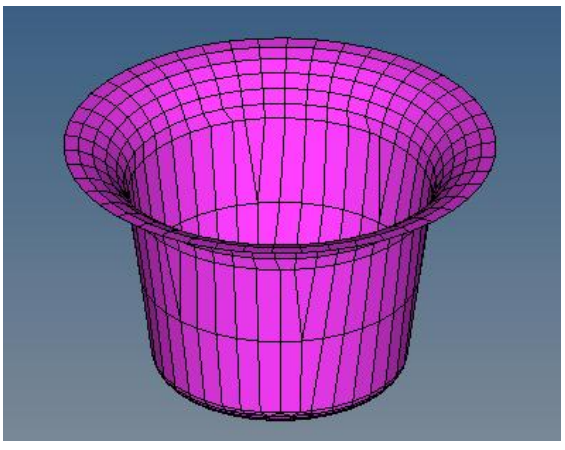

(b) Punch

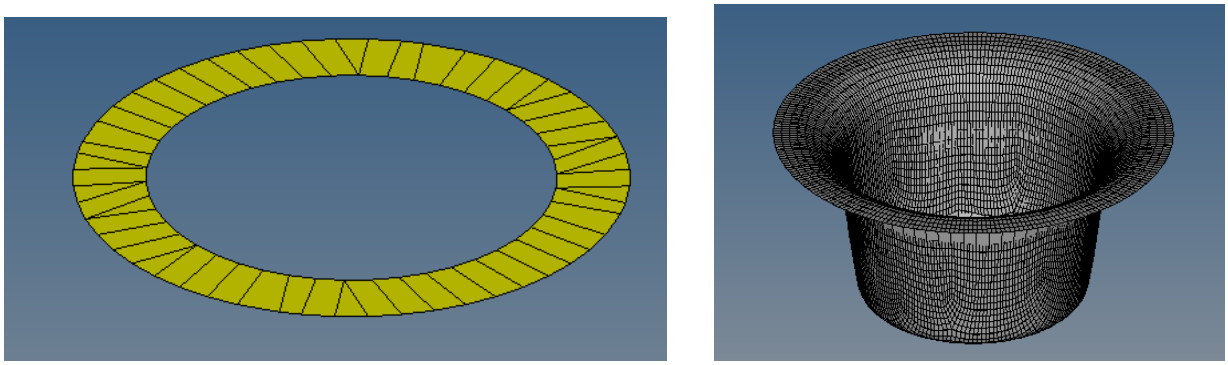

(c) Binder **(d) Blank**

Fig. 4.17: Meshes of (a) Die (b) Punch (c) Binder (d) Blank

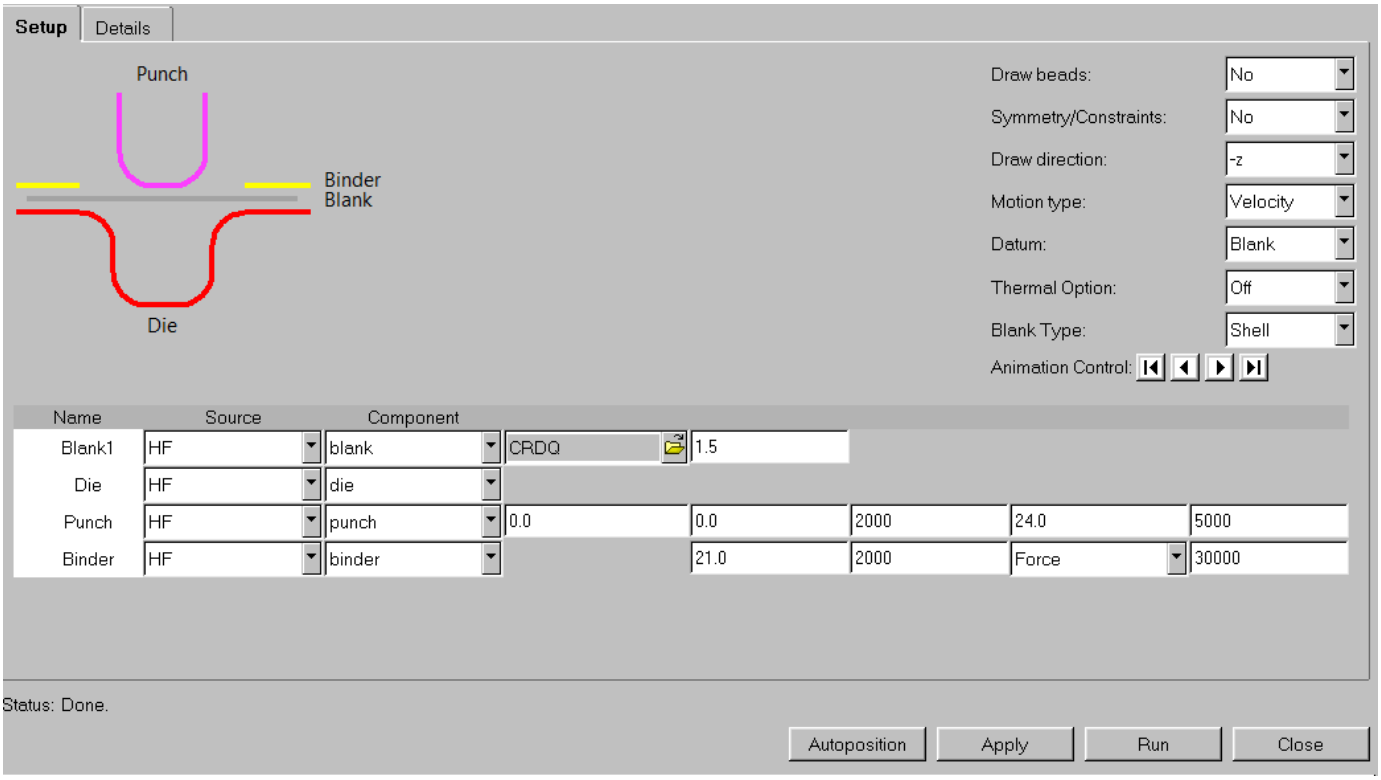

Fig. 4.18: Third stage Auto Process window

CHAPTER 5

RESULTS AND DISCUSSION

5.1 One-Step

The following figure gives the optimum size of a rectangular sheet out of which a blank of an appropriate size can be cut.

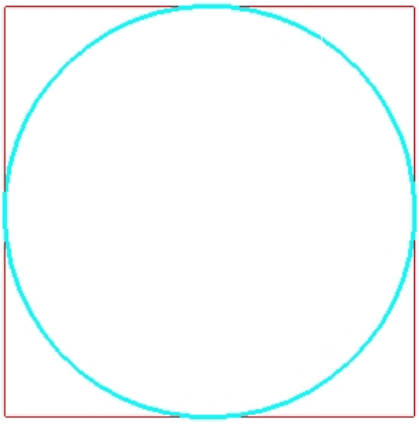

Rectangular Blank
Dimensions: 128.00 x 127.89 mm
Surface area: 16370.6 mm^2
Material: CRDQ Steel
Thickness: 1.50 mm
Mass: 0.194 kg
Unit cost: $ 0.14
Material utilization: 78.9642 %

Fig. 5.1: Blank Fit

Hyperform One-Step estimates the initial blank diameter to be 128mm but the blank diameter calculated according to [37] is as follows:

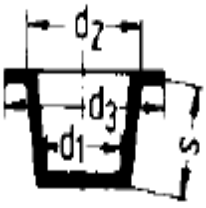

$$D = \sqrt{d_1^2 + 2s(d_1 + d_2) + d_3^2 - d_2^2}$$

Therefore, D comes out to be 134 mm. The difference between the blank diameters is due to the fact that Hyperform One-Step takes the blank material into account whereas the calculations are

based on the fact that the volume of the blank must be equal to the volume of the drawn component.

But, we take blank diameter to be 125mm because the first stage products drawn from 128 mm and 126 mm blank are wrinkled, no matter how much blank holder force is applied.

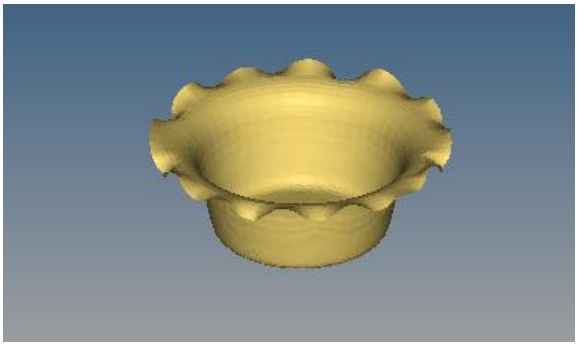

(a) BHF=30 KN

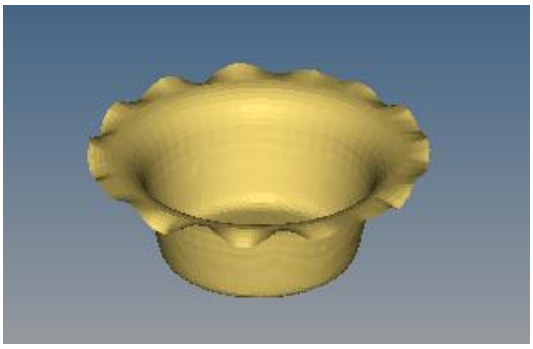

(b) BHF= 50KN

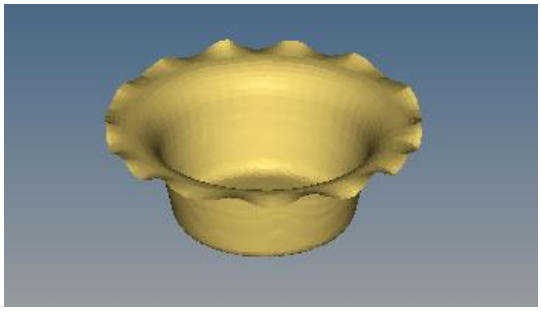

(c) BHF= 100 KN

Fig. 5.2: Stage one wrinkled products from blank diameter 128 mm

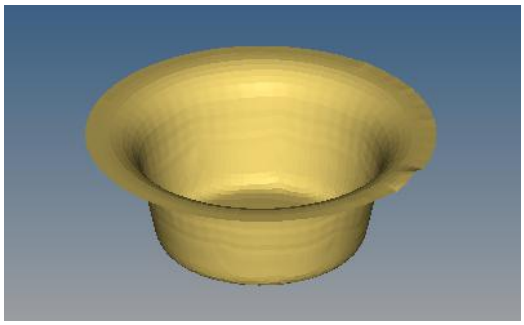

(a) BHF= 30 KN

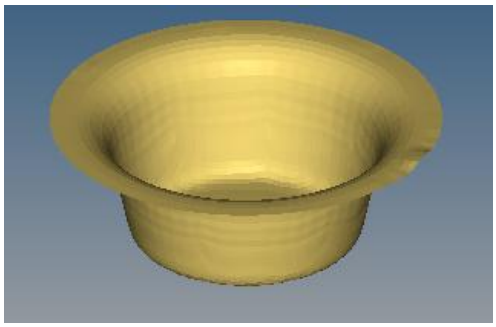

(b) BHF=50 KN

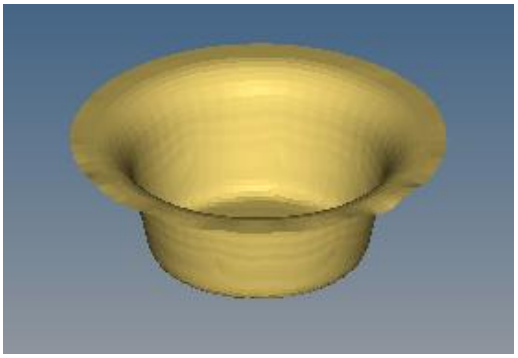

(c) BHF= 100 KN

Fig. 5.3: Stage one wrinkled products from blank diameter 126 mm

Fig. 5.4 shows the thinning percentage contour in the potential deep drawn part. As we can see the thinning percentage is greater than 22.30% in some areas and the maximum thinning percentage being 25.50%. This is due to the fact that the depth of draw is greater than the diameter and indicates that the part cannot be drawn in a single stage. Same results are predicted by the FLD zone contour and FLD in figures 5.5 and 5.6 respectively.

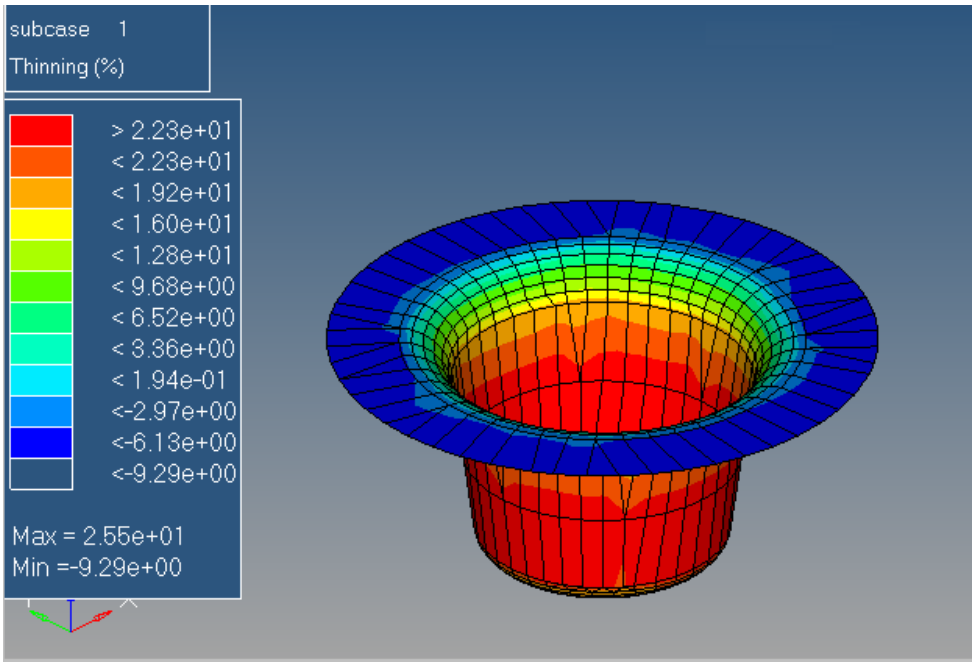

Fig. 5.4: Thinning % age contour

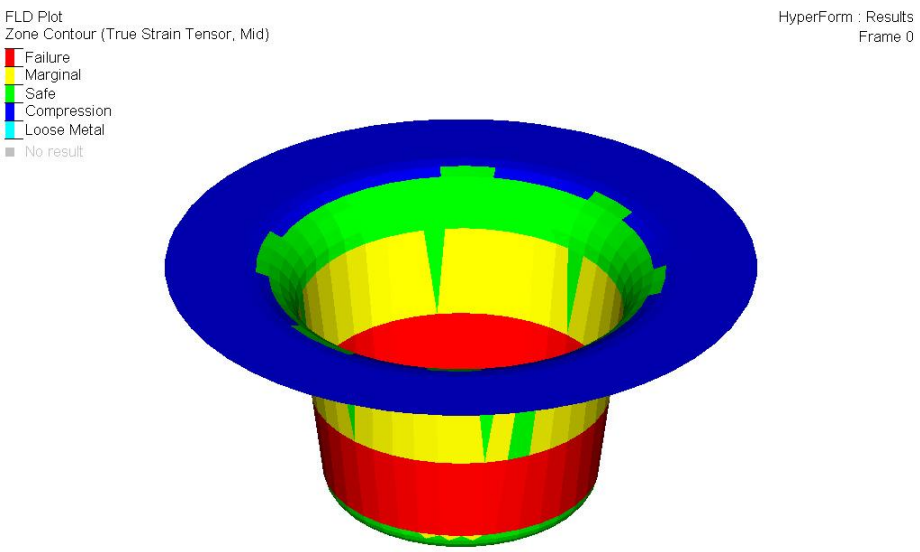

Fig. 5.5: FLD Plot Contour

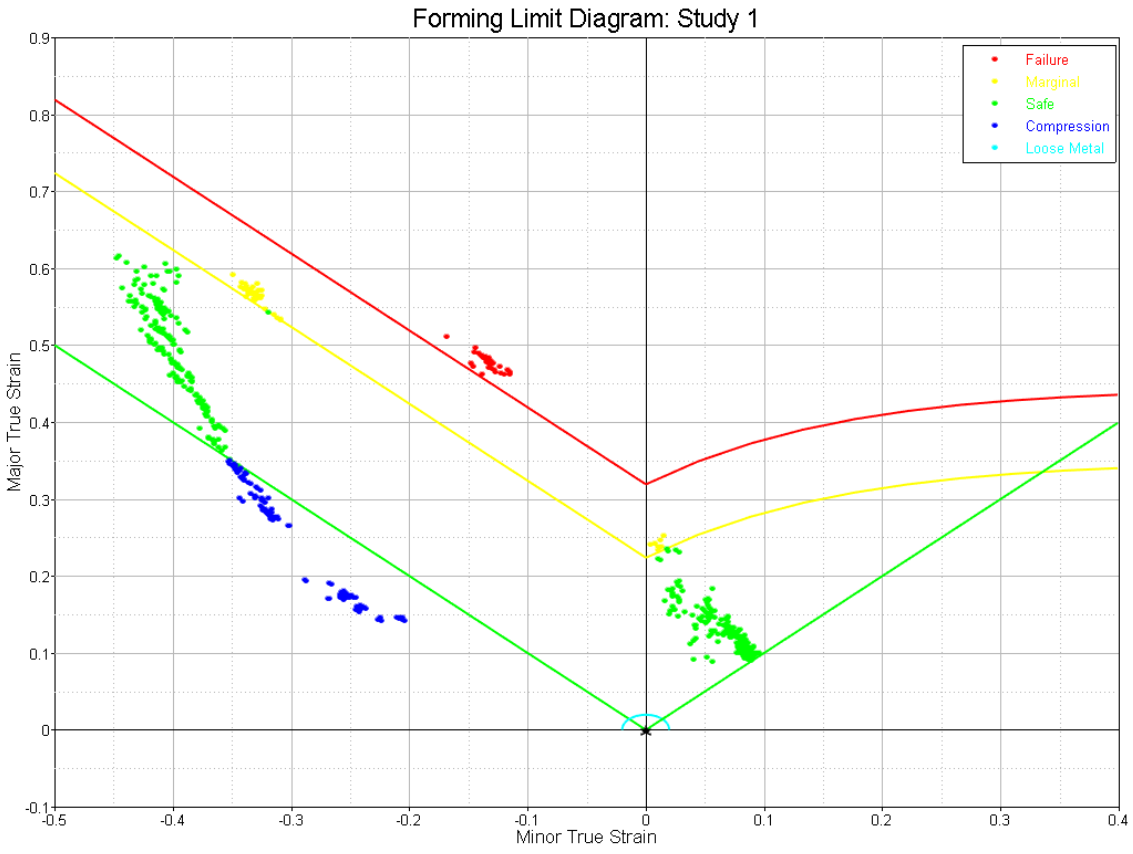

Fig. 5.6: Forming Limit diagram

5.2 Incremental

5.1.1 Stage One

Simulations were carried out to ascertain the depth of first draw with as low as possible thinning %. The first stage depth should be as large as possible because large depths cannot be obtained in subsequent stages because of strain hardening after the first stage. Simulations were carried out for three depths- 38 mm, 36 mm and 34 mm, keeping blank holder force at 30 KN.

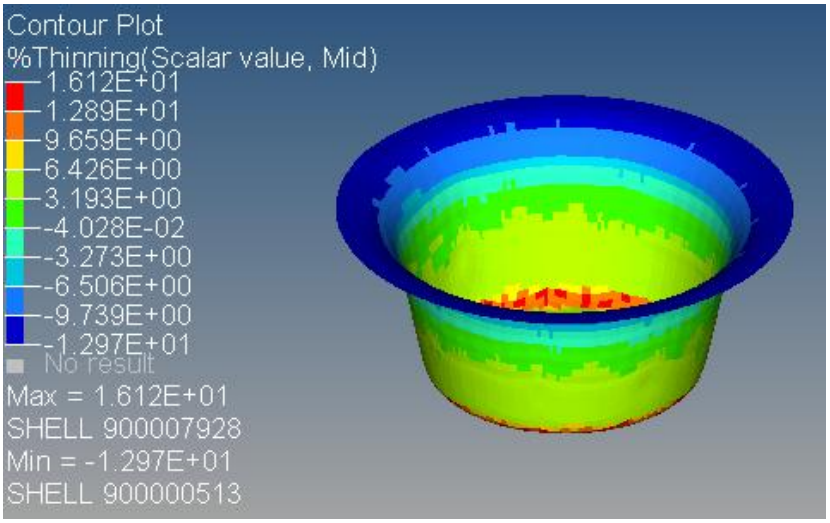

Fig. 5.7: Thinning percentage countour for stage one product with depth 38 mm

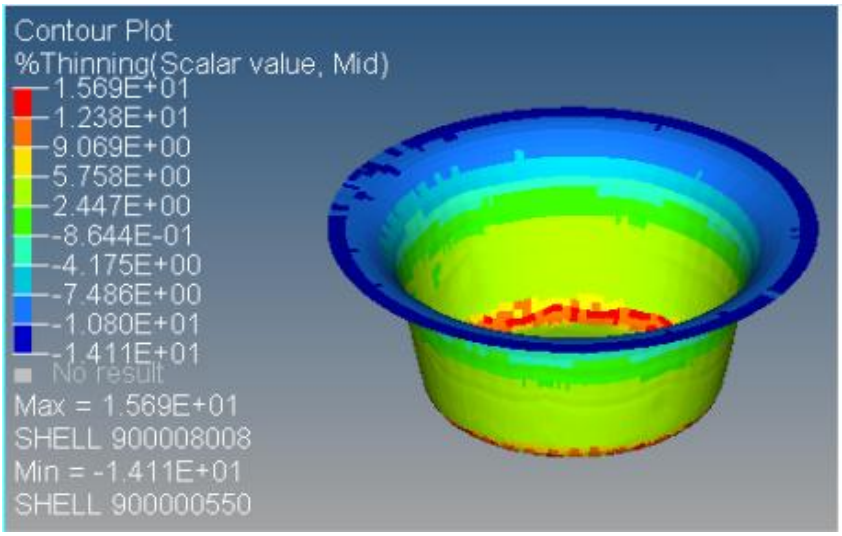

Fig. 5.8: Thinning percentage countour for stage one product with depth 36 mm

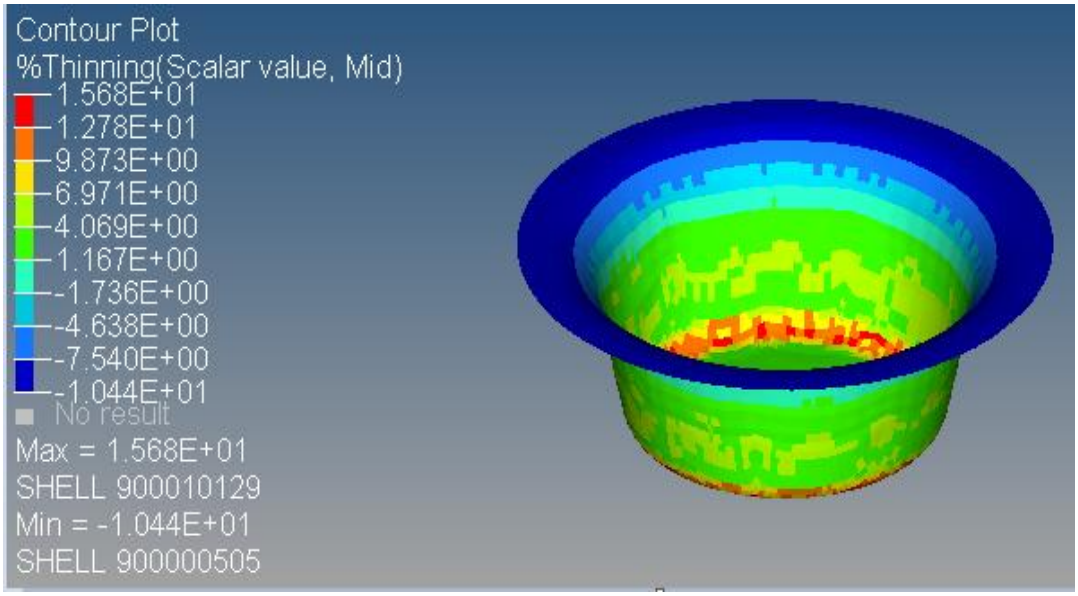

Fig. 5.9: Thinning percentage countour for stage one product with depth 34 mm

The products formed after first stage with depths of 38 mm and 36 mm have slight wrinkles, and though their maximum thinning percentage is only slightly more than that in the product with depth 34 mm, the width of the flange in 38 mm and 36 mm depth products is less than that in the case of 34 mm depth. Therefore, first stage depth has been chosen as 34 mm.

The thinning percentage contour for depth 34mm shows that the product formed after first stage of drawing does not have any areas where thinning percentage exceeds 15.68%, which is below the acceptable limit of 20% thinning. Therefore we can say that the product is free of tears and there is no possibility of a fracture due to the drawing process.

The forming limit diagram shows that the elements are distributed in safe zone and compression zone. The elements in the compression zone are near to the safe zone boundary which indicates that there is no wrinkling tendency.

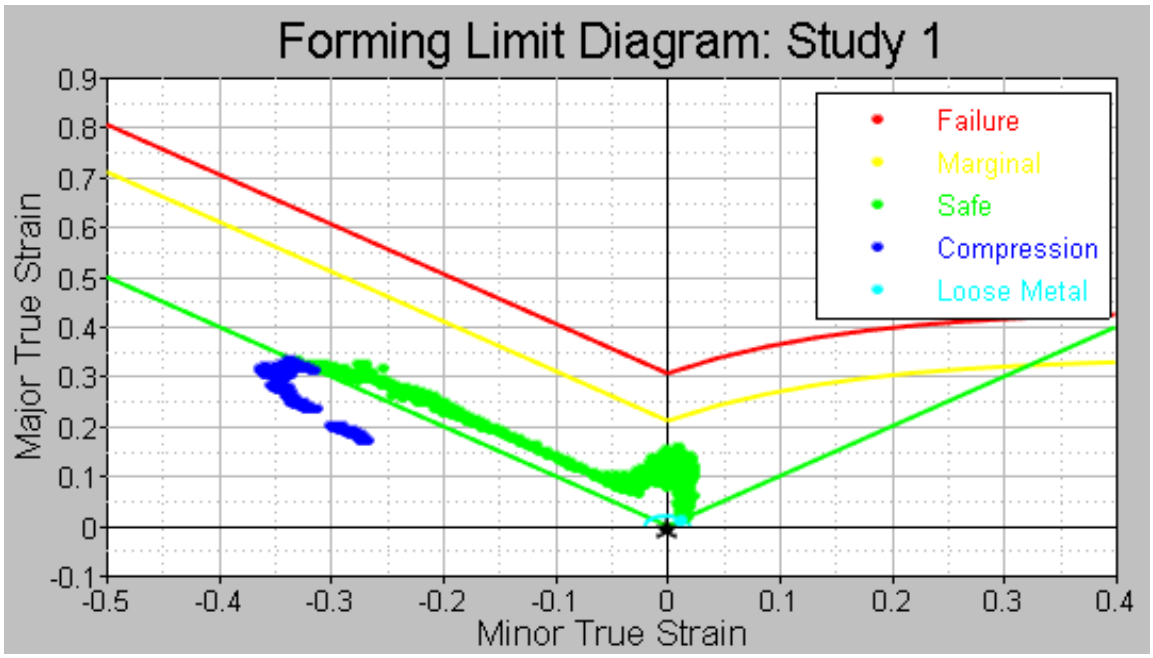

Fig. 5.10: Forming Limit Diagram for stage one product with 34 mm

5.1.2 Stage Two

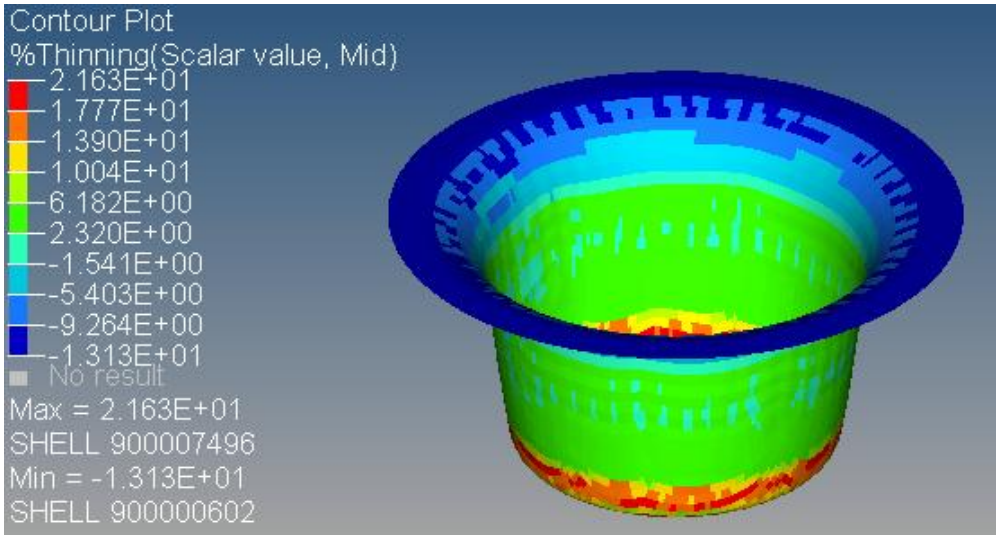

Fig. 5.11: Thinning percentage contour for stage two product with die radius 10 mm

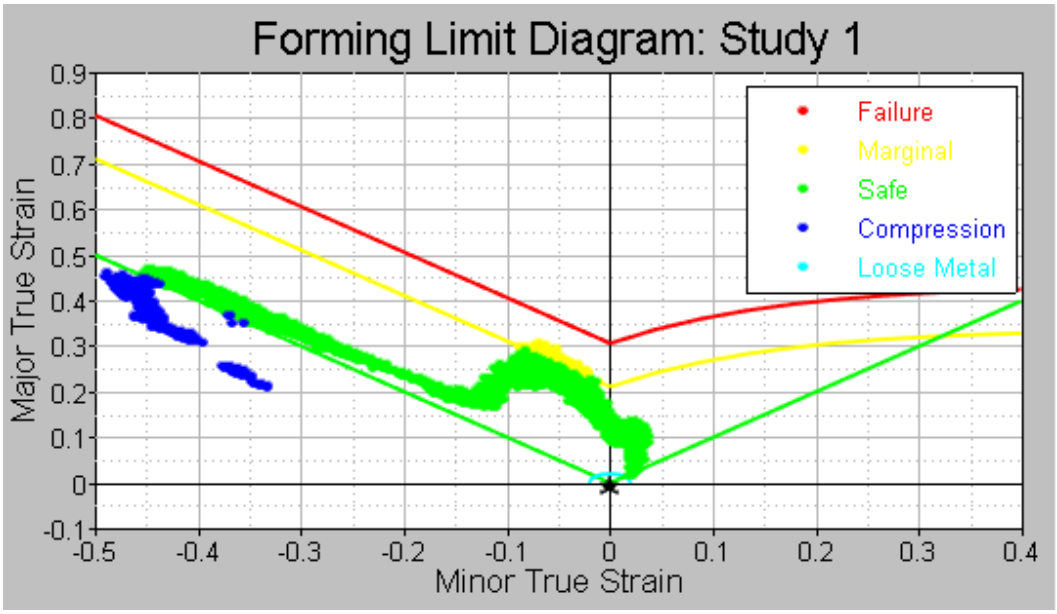

Fig. 5.12: Forming Limit Diagram for stage two product with die radius 10 mm

As it can be seen from the thinning percentage contour, the maximum thinning percentage is 21.63% which is a little over the acceptable limit of 20%. However, the Forming Limit Diagram doesn't show any elements failing, though there are some which are in the marginal safety region.

This above 20% thinning can be attributed to various factors, the main ones being high blank holder force, small die radius or depth of the drawn part. Therefore, to try to decrease the thinning to below 20%, more simulations are carried out for second stage.

Since the die radius is already sufficiently large, any further increase can lead to wrinkling tendency, but more importantly pull material from the flange region into the side wall region. Any further decrease in the die radius will only increase thinning percentage as depicted in fig. 5.13. Simulations for increased die radii have been carried out which have not yielded any major changes i.e. thinning has decreased by a very small decimal percentage. Therefore, no change is made to the die radius of 10 mm.

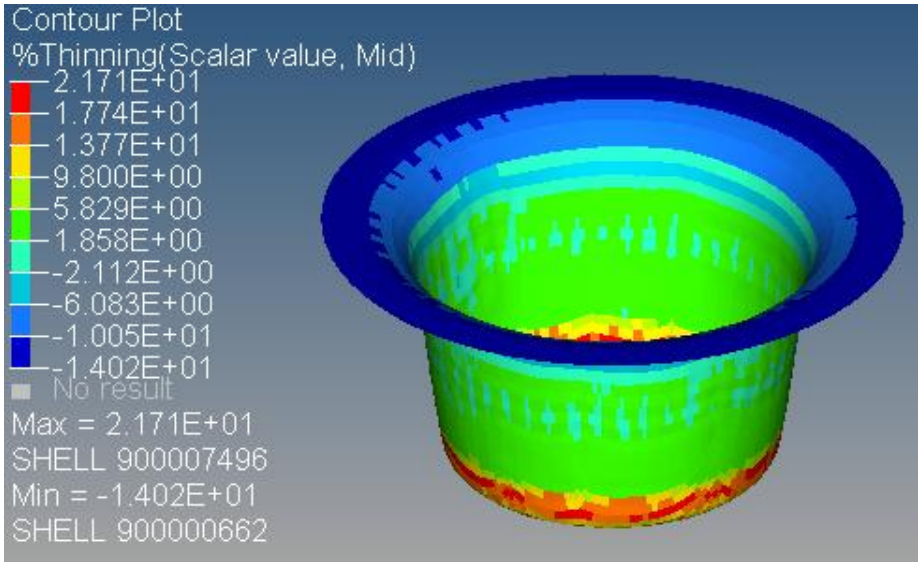

Fig. 5.13: Thinning percentage contour for stage two product with die radius 9 mm

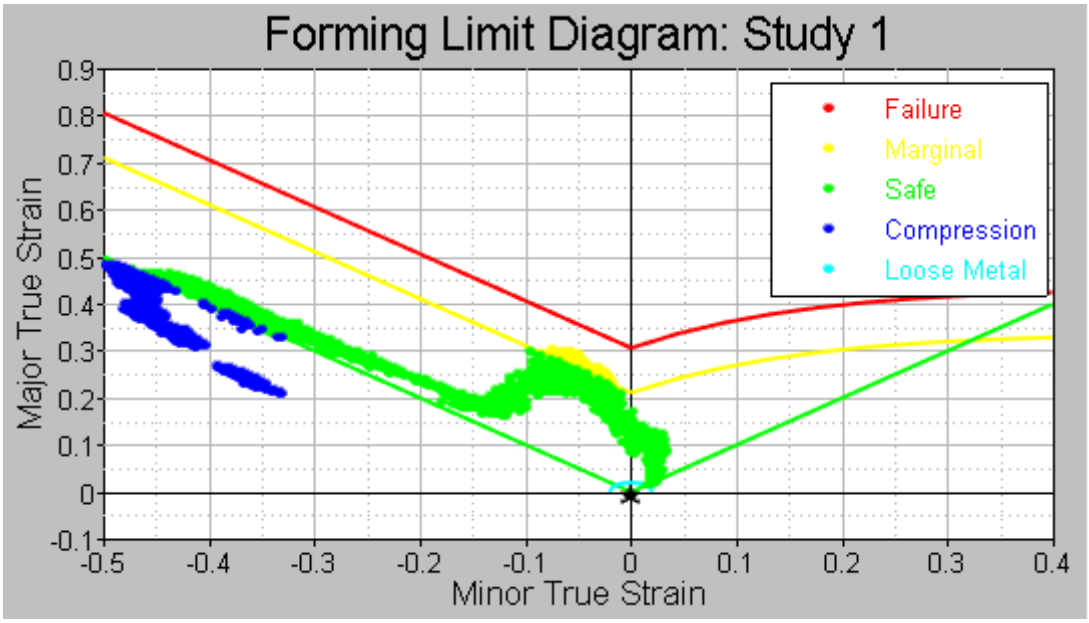

Fig. 5.14: Forming Limit Diagram for stage two product with die radius 9 mm

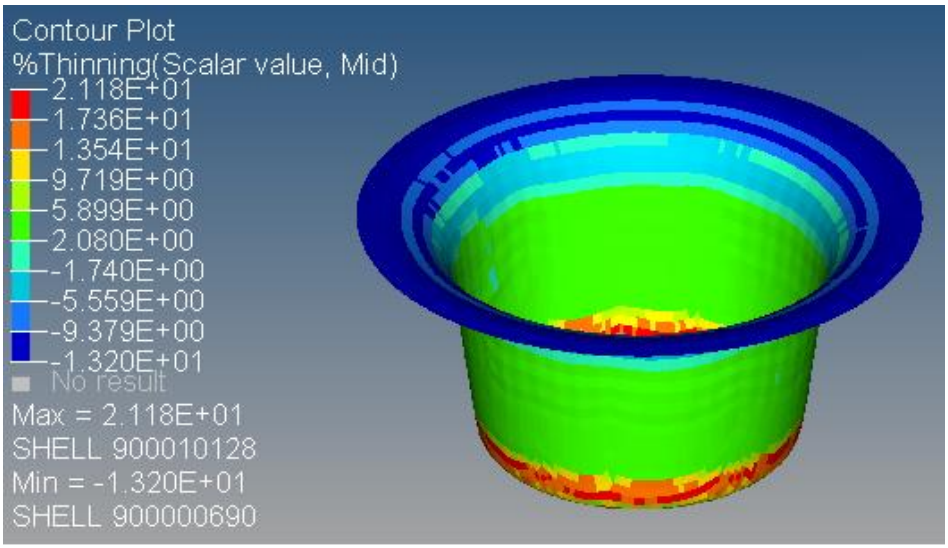

Fig. 5.15: Thinning percentage contour for stage two product with die radius 11 mm

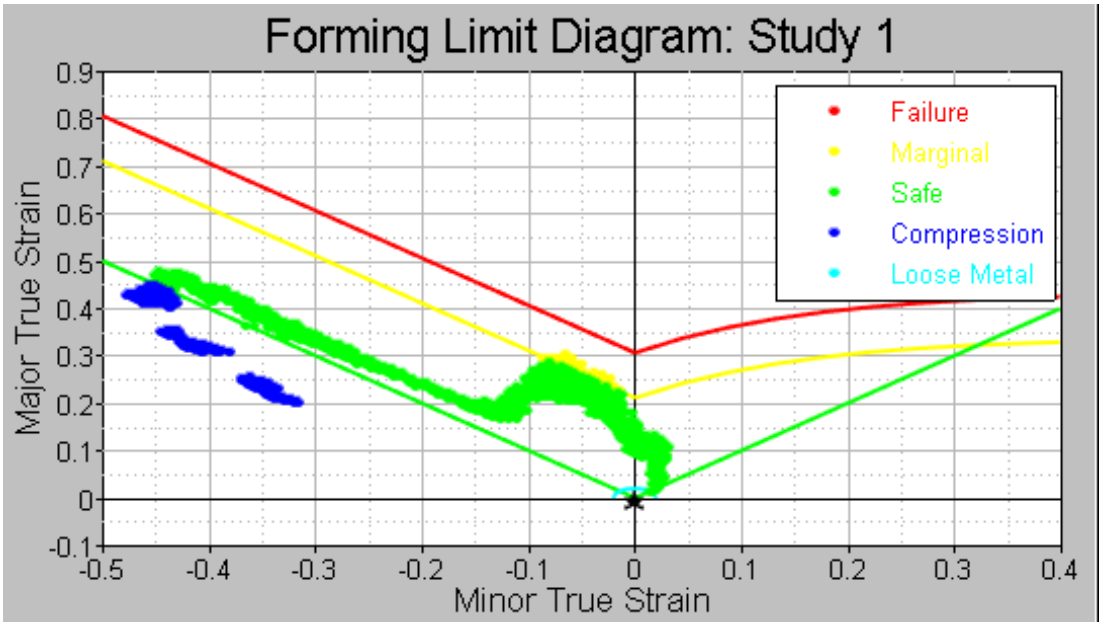

Fig. 5.16: Forming Limit Diagram for stage two product with die radius 11 mm

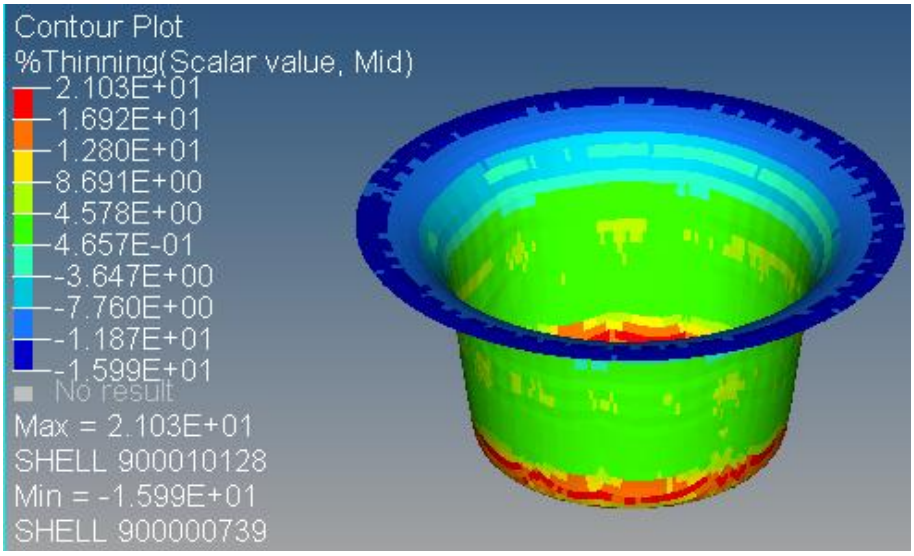

Fig. 5.17: Thinning percentage contour for stage two product with die radius 12 mm

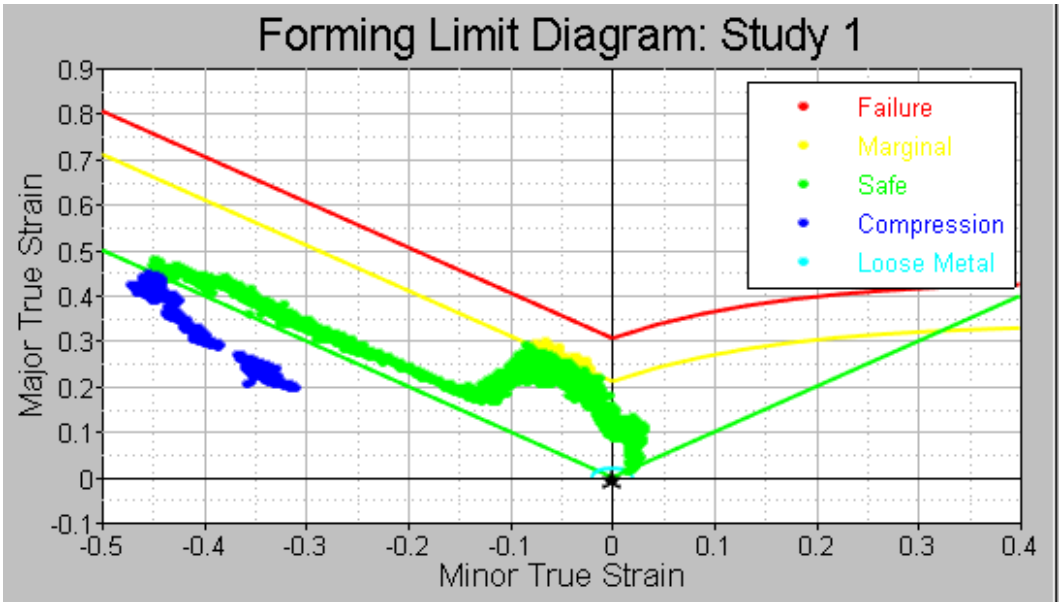

Fig. 5.18: Forming Limit Diagram for stage two product with die radius 12 mm

A simulation is done with reduced blank holder pressure equal to 25 KN from the previously applied 30 KN. The results don't show any positive effect of reducing the blank holder pressure as maximum thinning percentage comes out to be 21.74%.

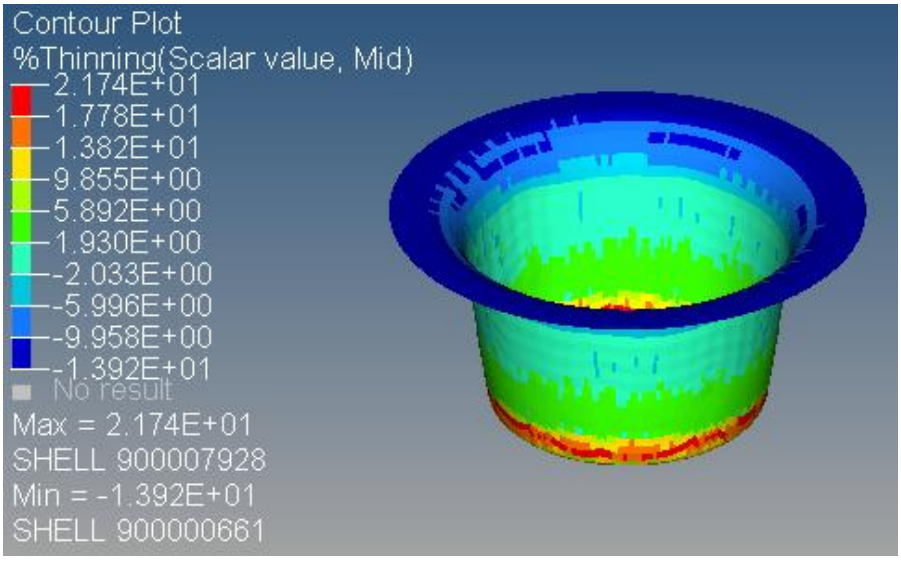

Fig. 5.19: Thinning percentage contour for stage two product with BHF=25 KN

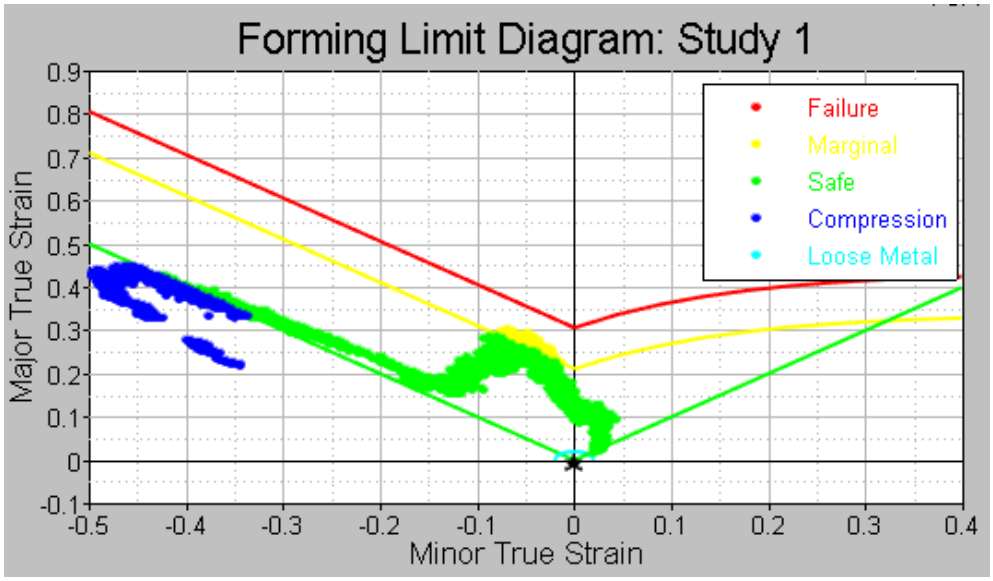

Fig. 5.20: Forming Limit Diagram for stage two product with BHF=25 KN

A simulation is done by reducing the height of the drawn part from 42 mm to 41 mm. Maximum thinning percentage only decreases by a very small decimal percentage to 21.60%.

These two alternative simulations by varying BHF and depth of drawn part do not prove to reduce the thinning below 20%, therefore we stick to our first simulation with BHF=30 KN and depth of drawn part 42 mm.

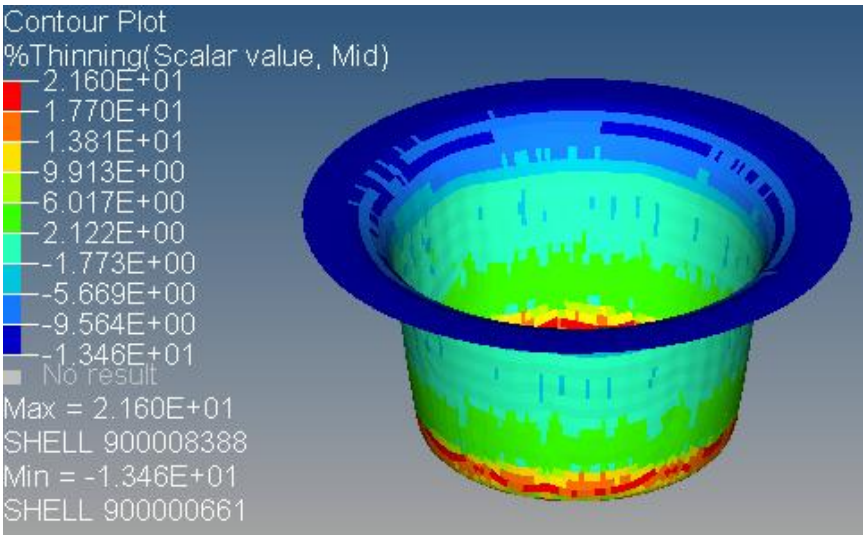

Fig. 5.21: Thinning percentage contour for stage two product with depth 41 mm

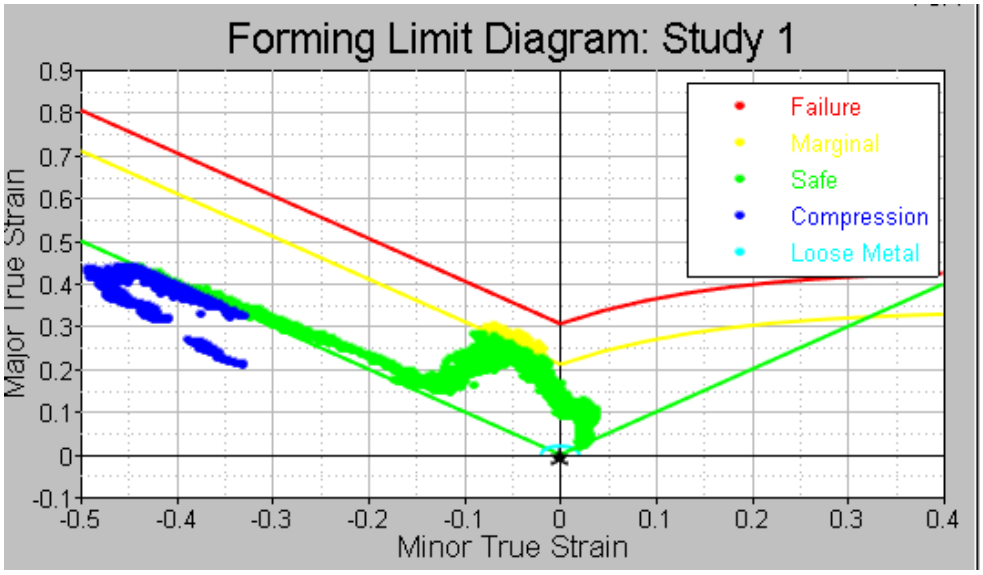

Fig. 5.22: Forming Limit Diagram for stage two product with depth 41 mm

5.1.3 Stage Three

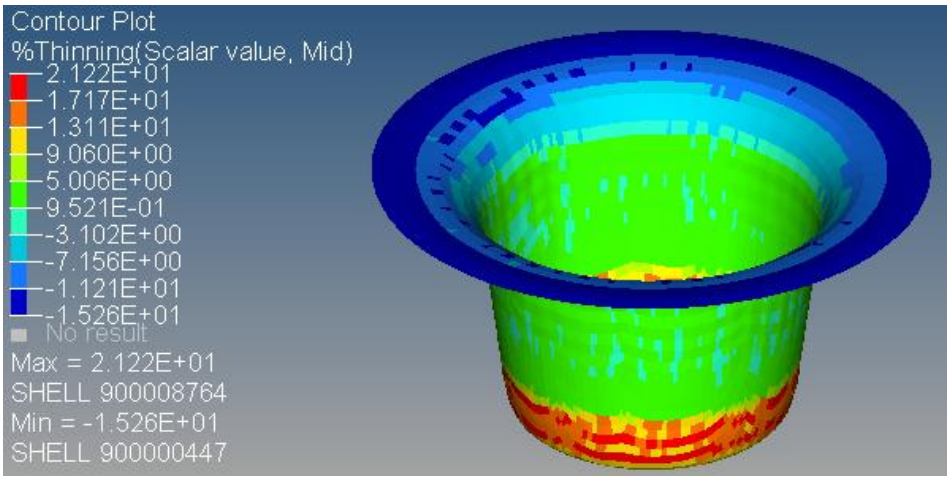

Fig. 5.23: Thinning percentage contour in stage three product

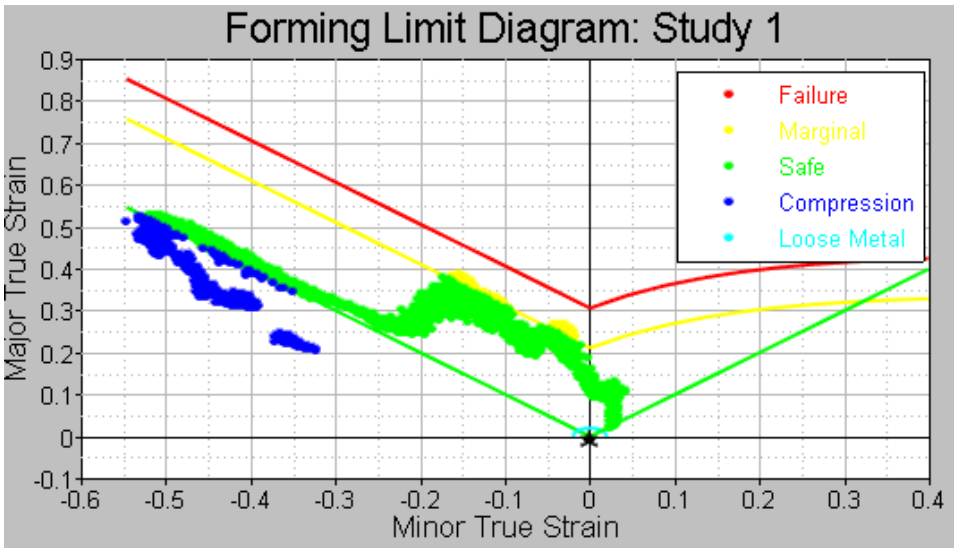

Fig. 5.24: Forming Limit Diagram for stage three product

Similar to the second stage, the maximum thinning percentage is a little above 20% i.e. 21.22%. However, again the Forming Limit Diagram doesn't show any failing elements, but again there are some in the marginal safety region.

CHAPTER 6

CONCLUSIONS AND FUTURE SCOPE

7.1 Conclusions

This dissertation work has been attempted to understand the deep drawing process through simulation only. Experimental work has not been done as the Altair Hyperform gives us the Forming Limit Diagrams, which are widely used to predict failure in drawn components. Radioss One-Step optimised the initial blank diameter to be 128 mm but a blank diameter of 125 mm was taken as the 128 mm blank was showing highly wrinkled products. Deep drawing was carried out in three stages using Radioss Incremental. The first stage product was defect free, but the second and third stage products showed a slight possibility of tear due to thinning. To ascertain the reason behind this extra thinning, alternative simulations were carried out for second stage, varying blank holder pressure, die radius and the depth to be drawn, but no positive effects were observed. Hence, the product with a little extra thinning was considered to be the final product.

7.2 Future Scope

The present analysis doesn't take springback into account, which can be analysed in the future. Also, constant blank holder pressure was used, but a number of studies nowadays are pointing towards varying blank holder pressure, which should certainly be applied to this model. The use of taper in the product has given high drawing ratios and this fact should be well exploited in the future.

REFERENCES

[1] John A. Schey, *"Introduction to Manufacturing Processes"*, Third Edition ed.: McGraw-Hill, 2000.

[2] Karl-Heinrich Grote and Erik K. Antonsson, "*Springer Handbook on Mechanical Engineering"*: Springer Science and Business Media, LLC New York, 2008.

[3] Serope Kalpakjian and Steven R. Schmid, *"Manufacturing Processes for Engineering Materials"*, Fourth Edition ed.: Prentice Hall, London, 2003.

[4] Serope Kalpakjian, Stephen Schmid, "*Manufacturing, Engineering and Technology*", SI 6th Edition, 2009

[5] Z. Marciniak, J.L. Duncan and S.J. Hu, "*"Mechanics of Sheet Metal Forming""*, Second Edition ed.: Butterworth-Heinemann, 2002.

[6] Hill, Rodney. *The mathematical theory of plasticity*. Vol. 11. Oxford university press, 1998.

[7] Chung, S. Y., and H. W. Swift. "Cup-drawing from a flat blank: part I. Experimental investigation." *Proceedings of the institution of mechanical engineers* 165.1 (1951): 199-211.

[8] Chung, S. Y., and H. W. Swift. "Cup-drawing from a flat blank: part II. Analytical investigation." *Proceedings of the institution of mechanical engineers* 165.1 (1951): 211-215

[9] Lankford, W. T., S. C. Snyder, and J. A. Bauscher. "New criteria for predicting the press performance of deep drawing sheets." *Trans. ASM* 42 (1950): 1197-1232.

[10] El-Sebaie, M. G., and P. B. Mellor. "Plastic instability conditions in the deep-drawing of a circular blank of sheet metal." *International Journal of Mechanical Sciences* 14.9 (1972): 535-540.

[11] Darendeliler, H., and B. Kaftanoglu. "Deformation analysis of deep-drawing by a finite element method." *CIRP Annals-Manufacturing Technology* 40.1 (1991): 281-284.

[12] Yang, D. Y., and H. S. Lee. "Analysis of three-dimensional deep drawing by the energy method." *International journal of mechanical sciences* 35.6 (1993): 491-516.

[13] Lee, C. H., and Shiro Kobayashi. "New solutions to rigid-plastic deformation problems using a matrix method." *Journal of Engineering for Industry* 95.3 (1973): 865-873.

[14] Seo, Young. "Simulation beats trial-and-error." *Metal Forming(USA)* 36.5 (2002): 32-34.

[15] Saran, Michal J., and Alf Samuelsson. "Elastic-viscoplastic implicit formulation for finite element simulation of complex sheet forming processes." *International journal for numerical methods in engineering* 30.8 (1990): 1675-1697.

[16] Jain, N., Shi, X., Ngaile, G., Altan, T., Pax, B., Harman, B., & Homan, G. (2003). Simulation Confirms Deep Drawn Die Design. *Metal Forming Magazine*, 51-56.

[17] Keeler, S. P.: Plastic instability and fracture in sheet stretched over rigid punches, Thesis, Massachusetts Institute of Technology, Boston, MA 1961.

[18] Keeler, Stuart Philip, and Walter A. Backofen. "Plastic instability and fracture in sheets stretched over rigid punches." *Asm Trans Q* 56.1 (1963):25-48.

[19] Goodwin, G. M.: Application of strain analysis to sheet metal forming problems in the press shop, Society of Automotive Engineers (1968), No. 680093, 380-387.

[20] Kaftanoglu, B. "Plastic analysis of flange wrinkling in axisymmetrical deep-drawing." *Proceedings of the Twenty-First International Machine Tool Design and Research Conference*. Macmillan Education UK, 1981.

[21] Ramaekers, J. A. H., A. de Winter, and M. W. H. Kessels. "" Deepdrawability of a Round Cylindrical Cup." *IDDRG*. Vol. 94. 1994.

[22] Cao, Jian, and M. C. Boyce. "A predictive tool for delaying wrinkling and tearing failures in sheet metal forming." *Journal of Engineering Materials and Technology* 119.4 (1997): 354-365.

[23] Kawka, M., Olejnik, L., Rosochowski, A., Sunaga, H., & Makinouchi, A. (2001). Simulation of wrinkling in sheet metal forming. *Journal of Materials Processing Technology*, *109*(3), 283-289.

[24] de Magalhães Correia, João Pedro, and Gérard Ferron. "Wrinkling predictions in the deep-drawing process of anisotropic metal sheets." *Journal of materials processing technology* 128.1 (2002): 178-190.

[25] El Sherbiny, M., H. Zein, and M. Abd-Rabou. "Thinning and residual stresses of sheet metal in the deep drawing process." *Materials & Design* 55 (2014): 869-879.

[26] Rees, D. W. A. "Factors influencing the FLD of automotive sheet metal."*Journal of materials processing technology* 118.1 (2001): 1-8.

[27] Faraji, Ghader, Mahmud M. Mashhadi, and Ramin Hashemi. "Using the finite element method for achieving an extra high limiting drawing ratio (LDR) of 9 for cylindrical components." *CIRP Journal of Manufacturing Science and Technology* 3.4 (2010): 262-267.

[28] Choubey, Ajay Kumar, Geeta Agnihotri, and C. Sasikumar. "Numerical Validation of Experimental Result in Deep-Drawing." *Materials Today: Proceedings* 2.4 (2015): 1951-1958.

[29] Dieter, George Ellwood, and David J. Bacon. *Mechanical metallurgy*. Vol. 3. New York: McGraw-Hill, 1986

[30] Suchy, Ivana. "*Handbook of die design*." (2006)

[31] Altan, Taylan, and A. Erman Tekkaya, eds. *Sheet metal forming: fundamentals*. Asm International, 2012.

[32] Erichsen, A. "A new test for thin sheets." *Stahl and Eisen* 34 (1914): 879-882.

[33] Pomey, G.: Formability of thin sheet (in French). (Vol.l-3), Collection I.R.S.I.D.-O.T.U.A., Paris 1976.

[34] Pomey, 0.; Parniere, P.: Formability of thin sheet (in French), Techniques de l'ingenieur (1980), Nr. 1, M 695,1-16, M 696,1-19.

[35] Banabic, Dorel. *Formability of metallic materials: plastic anisotropy, formability testing, forming limits*. Springer Science & Business Media, 2000.

[36] Fukui, S.: *Researches on the deep-drawing process*, Scientific Papers of the I. P. C. R. 34 (1939), 1422-1527.

[37] Lange, Kurt. "*Handbook of metal forming*." McGraw-Hill Book Company, 1985, (1985):828.